Aus dem Institut für Schlaganfall- und Demenzforschung (ISD)
Klinik der Universität München
Direktor: Prof. Dr. Martin Dichgans


# *The atypical chemokine MIF and B lymphocytes in atherosclerosis: emerging molecular and cellular links*

Dissertation
zum Erwerb des Doktorgrades der Medizin
an der Medizinischen Fakultät
der Ludwig-Maximilians-Universität zu München

vorgelegt von
Sabrina Gabriele Reichl

aus
Nürnberg

Jahr
2023

Mit Genehmigung der Medizinischen Fakultät
der Universität München

| | |
|---|---|
| Berichterstatter: | Prof. Dr. Jürgen Bernhagen |
| Mitberichterstatter: | Prof. Dr. Alexander Bartelt<br>PD Dr. Andreas Herbst |
| Mitbetreuung durch den promovierten Mitarbeiter: | Dr. Omar El Bounkari |
| Dekan: | Prof. Dr. med. Thomas Gudermann |
| Tag der mündlichen Prüfung: | 30.11.2023 |

# Table of Contents

# Published Manuscripts

Results and methods specified in this thesis were published in part in the following manuscripts, on which I am a key contributing author:

Krammer C, Yang B, **Reichl S**, Besson-Girard S, Ji H, Bolini V, Schulte C, Noels H, Schlepckow K, Jocher G, Werner G, Willem M, El Bounkari O, Kapurniotu A, Gokce O, Weber C, Mohanta S, Bernhagen J. Pathways linking aging and atheroprotection in *Mif*-deficient atherosclerotic mice. ***FASEB J.*** 2023 Mar;37(3):e22752.

Krammer C, Yang B, **Reichl S**, Bolini V, Schulte C, Noels H, El Bounkari O, Kapurniotu A, Weber C, Mohanta S, Bernhagen J. Link between aging and atheroprotection in *Mif*-deficient atherosclerotic mice. ***bioRxiv*** 2021.12.14.471281.

Krammer C. MIF proteins and their receptors in atherogenesis: Structure-activity relationships and novel cellular routes. ***Dissertation, LMU München: Medizinische Fakultät.*** 2021. Appendix A: Publication III.

# Zusammenfassung

Macrophage migration inhibitory factor (MIF) ist ein entzündliches Zytokin und atypisches Chemokin (ACK), das in atherosklerotischen Läsionen beim Menschen stark hochreguliert ist und mit koronarer Herzerkrankung korreliert. MIF ist ein kausaler Faktor der Atherogenese, wie in atherogenen Mausmodellen mittels genetischer Deletion oder Antikörperblockade gezeigt. Die pro-atherogenen Effekte von MIF werden hauptsächlich durch die Bindung an die klassischen Chemokinrezeptoren CXCR2 und CXCR4 und die damit verbundene Rekrutierung von Monozyten und T-Zellen gesteuert.

In jüngster Zeit wurde auch B-Zellen eine wichtige Rolle in der Atherogenese zugeschrieben. Inzwischen sind unterschiedliche B-Zell-Subpopulationen bekannt – die atheroprotektiven B1-Zellen und die pro-atherogenen B2-Zellen. Während nur wenige B-Zellen in atherosklerotischen Plaques zu finden sind, sammelt sich der Großteil in der Adventitia der brachiocephalen Arterie (BCA) und der abdominellen Aorta (AA). In alten, atherosklerotischen *Apoe-/-* Mäusen wurden B-Zellen vermehrt in sogenannten Artery Tertiary Lymphoid Organs (ATLOs) nachgewiesen. ATLOs sind lymphoidartige Organe in der Adventitia der arteriellen Wand, in der Nähe von atherogenen Prädilektionsstellen, und können als Zentren lokaler humoraler Immunität angesehen werden. Man nimmt an, dass in ATLOs lokalisierte B-Zellen einen vorwiegend atheroprotektiven Phänotyp aufweisen.

Die Verbindung zwischen B-Zellen und MIF in der Atherogenese sowie altersbedingte Veränderungen waren bisher unklar. In meiner Doktorarbeit habe ich den Einfluss einer globalen *Mif*-Defizienz auf atherosklerotische *Apoe-/-* Mäuse in verschiedenen Altersstufen und unter einer cholesterin- und fettreichen Diät untersucht, mit Fokus auf vaskulärer Atheroprotektion und ATLO-ähnlicher B-Zell-Formierung.

Die Daten zeigen einen lokoregionären, atheroprotektiven Phänotyp bei 30 Wochen alten, für 24 Wochen fettreich-gefütterten, *Apoe-/- Mif-/-* Mäusen, welcher mit dem Alterungsprozess verloren ging. Als zugrunde liegende Ursache konnten folgende Mechanismen identifiziert werden:

i) B-Zell-Cluster, die Merkmale früher ATLOs aufweisen, wurden in vergleichsweise jungen *Apoe-/- Mif-/-* Mäusen, aber nicht in *Apoe-/-* Kontrollmäusen, nachgewiesen, was darauf hindeutet, dass die Abwesenheit des *Mif*-Gens die Ausbildung von ATLO-ähnlichen Clustern in solchen pro-atherogenen Mäusen beschleunigt.

ii) Plasmaspiegel von atheroprotektiven anti-oxLDL IgM Antikörpern waren bei alten *Apoe-/- Mif-/-* Mäusen im Vergleich zu *Apoe-/-* Kontrollmäusen verringert.

iii) Die Anzahl pro-atherogener CD4+ T-Zellen in der Milz war erhöht unter *Mif*-Defizienz und in fortgeschrittenem Alter.

Die Ergebnisse geben Einblick in die komplexe Verbindung zwischen MIF und B-Lymphozyten in der Pathogenese der Atherosklerose und beleuchten altersbedingte Effekte, die bei der Entwicklung MIF-basierter Therapieoptionen zu berücksichtigen sind.

# Abstract

Macrophage migration inhibitory factor (MIF) is an inflammatory mediator and non-canonical (aka atypical) chemokine (ACK) that is enriched in atherosclerotic lesions in humans and that shows a correlation with coronary artery disease (CAD). MIF plays a crucial role in atherogenesis as demonstrated in experimental atherosclerosis studies utilizing *Mif* gene deletion or antibody neutralization. The atherogenic effects of MIF mainly arise from its interaction with the canonical chemokine receptors CXCR2 and CXCR4, thereby mediating lesional recruitment of monocytes and T lymphocytes, respectively.

B lymphocytes have also emerged as drivers in the atherosclerotic disease process with subtype-dependent effects. B1 B cells are considered to be atheroprotective, whereas B2 B cells exacerbate atherosclerosis. While only a few B cells appear in atherosclerotic plaques, the majority accumulates in the adventitia of innominate artery (BCA) and abdominal aorta (AA). In highly aged hyperlipidemic genetically predisposed mice, B cells have been detected within artery tertiary lymphoid organs (ATLOs). These are lymphoid aggregates in the adventitia of the arterial wall, close to inflammation sites, and can be considered as centers of local humoral immunity. B cells derived from ATLOs have been associated with atherogenesis-cushioning functions.

However, links between B cells and MIF in atherogenesis as well as age-related changes have been elusive. I my MD thesis, I have analyzed the effect of global *Mif* deletion on pro-atherogenic *Apoe-/-* mice throughout various stages of aging and cholesterol-rich high-fat diet (HFD) focusing on vascular site-specific atheroprotection and ATLO-like B cell clustering.

The data suggest a regio-specific atheroprotective phenotype in 30-week-old *Apoe-/- Mif-/-* mice on HFD for 24 weeks, which was lost during the process of aging. As underlying cause, the following mechanisms could be identified:

i) B cell-rich clusters harboring hallmarks of early ATLOs were detected in relatively younger *Apoe-/- Mif-/-* mice but not *Apoe-/-* mice without *Mif* deletion, indicating that the absence of the *Mif* gene speeds up the development of ATLO-like clusters in these animals.

ii) Atheroprotective plasma anti-oxLDL IgM antibody titers were decreased in older *Apoe-/- Mif-/-* mice compared to *Apoe-/-* control mice.

iii) Atheroprogressive CD4+ T cell counts in spleen were increased upon *Mif*-deficiency and aging.

The results give insight into the complex connection between MIF and lymphocytes of the B lineage in atherosclerotic pathology and unravel age-related effects that should be considered when developing MIF-targeted approaches.

# List of Figures

# List of Tables

# Abbreviations

| | |
|---|---|
| **%** | **Percent** |
| **°C** | Degree Celsius |
| **µg** | Microgram |
| **µl** | Microliter |
| **µM** | Micromolar |
| **µm** | Micrometer |
| **AA** | Abdominal aorta |
| **ACK** | Atypical chemokine |
| **ACS** | Acute coronary syndrome |
| **AF488/647** | Alexa Fluor 488/647 |
| **AMP** | Adenosine monophosphate |
| **AMPK** | AMP-activating protein kinase |
| **APC** | Allophycocyanin |
| **APC-Cy7** | Allophycocyanin-cyanine 7 |
| **Apoe** | Apolipoprotein e |
| **ATLO** | Artery tertiary lymphoid organ |
| **ATP** | Adenosine triphosphate |
| **BAFF** | B cell activating factor |
| **BCA** | Brachiocephalic artery |
| **BCR** | B cell receptor |
| **BM** | Bone marrow |
| **Breg** | Regulatory B cell |
| **BSA** | Bovine serum albumin |
| **BTK** | Bruton tyrosine kinase |
| **CAD** | Coronary artery disease |
| **CD** | Cluster of differentiation |
| ***C*-terminal** | Carboxy-terminal |
| **CVD** | Cardiovascular disease |
| **Cy3/5** | Cyanine 3/5 |
| **DAPI** | 4’,6-Diamidino-2-phenylindole |

| | |
|---|---|
| **DC** | Dendritic cell |
| **dd$H_2O$** | Double-distilled water |
| **D-DT** | D-dopachrome tautomerase |
| **dl** | Deciliter |
| **Ebf1** | Early B cell factor 1 |
| **EC** | Endothelial cell |
| **EDTA** | Ethylenediaminetetraacetic acid |
| **ELISA** | Enzyme-linked immunosorbent assay |
| **ERK** | Extracellular signal-regulated kinase |
| **Fab** | Antigen-binding fragment |
| **FACS** | Fluorescence-activated cell sorting |
| **Fc** | Crystallizable fragment |
| **FDC** | Follicular dendritic cell |
| **FITC** | Fluorescein isothiocyanate |
| **FO B cell** | Follicular B cell |
| **g** | Acceleration of gravity |
| | Gram |
| **GC** | Germinal center |
| **GM-CSF** | Granulocyte-macrophage colony-stimulating factor |
| **GPCR** | G-protein-coupled receptor |
| **h** | Hour |
| **H-chain** | Immunoglobulin heavy chain |
| **HCT** | Hematocrit |
| **H&E** | Hematoxylin-Eosin |
| **HEV** | High endothelial venule |
| **HFD** | High-fat diet |
| **HGB** | Hemoglobin |
| **HMGB1** | High mobility group box protein 1 |
| **HRP** | Horseradish peroxidase |
| **HSC** | Hematopoietic stem cell |
| **IFN-γ** | Interferon-γ |

| | |
|---|---|
| **Ig** | Immunoglobulin |
| **IL** | Interleukin |
| **IRA** | Innate response activator |
| **ISO-1** | (S,R)-3-(4-hydroxyphenyl)-4,5-dihydro-5-isoxazole acetic acid methyl ester |
| **JNK** | c-Jun *N*-terminal kinase |
| **kg** | Kilogram |
| **LAAS** | Large artery atherosclerotic stroke |
| **L-chain** | Immunoglobulin light chain |
| **LDL** | Low-density lipoprotein |
| **Ldlr** | Low-density lipoprotein receptor |
| **LN** | Lymph node |
| **LPS** | Lipopolysaccharide |
| **Ly6G** | Lymphocyte antigen 6 complex locus G6D |
| **Lyve-1** | Lymphatic vessel endothelial hyaluronic acid receptor |
| **M** | Molar |
| **MAPK** | Mitogen-activated protein kinase |
| **MCH** | Mean corpuscular hemoglobin |
| **MCHC** | Mean corpuscular hemoglobin concentration |
| **MCP-1** | Monocyte chemoattractant protein-1 |
| **M-CSF** | Macrophage colony-stimulating factor |
| **MCV** | Mean corpuscular volume |
| **mg** | Milligram |
| **MHC** | Major histocompatibility complex |
| **MI** | Myocardial infarction |
| **MIF** | Macrophage migration inhibitory factor |
| **min** | Minutes |
| **ml** | Milliliter |
| **mM** | Millimolar |
| **mm** | Millimeter |
| **MMF** | Medetomidine, midazolam and fentanyl |
| **MMP** | Matrix metalloproteinase |

| | |
|---|---|
| **MPV** | Mean platelet volume |
| **MS** | Multiple sclerosis |
| **MZ B cell** | Marginal zone B cell |
| **n** | Quantity |
| **Nf-κB** | Nuclear factor 'kappa-light-chain-enhancer' of activated B cells |
| **nm** | Nanometer |
| **ns** | non-significant |
| ***N*-terminal** | Amino-terminal |
| **ORO** | Oil-Red-O |
| **OSE** | Oxidation-specific epitope |
| **oxLDL** | Oxidized low-density lipoprotein |
| **P** | *P* value |
| **Pax5** | Paired box gene 5 |
| **PBS** | Phosphate-buffered saline |
| **PE** | Phycoerythrin |
| **PE-Cy7** | Phycoerythrin-cyanine 7 |
| **PerCP-Cy5.5** | Peridinin chlorophyll protein-cyanine 5.5 |
| **PFA** | Paraformaldehyde |
| **pH** | Potentia hydrogenii |
| **PI3K** | Phosphoinositide 3-kinase |
| **PNAd** | Peripheral node addressin |
| **PRR** | Pattern recognition receptor |
| **Rag1/2** | Recombination-activating enzyme 1/2 |
| **REA** | Recombinant engineered antibody |
| **RBC** | Red blood cell |
| **RDW** | Red blood cell distribution width |
| **RT** | Room temperature |
| **SD** | Standard deviation |
| **sec** | Seconds |
| **SLE** | Systemic lupus erythematosus |
| **SLO** | Secondary lymphoid organ |

| | |
|---|---|
| **SMC** | Smooth muscle cell |
| **T1/2 B cell** | Transitional type 1/2 B cell |
| **Th cell** | T-helper cell |
| **TMB** | 3,3',5,5'-tetramethylbenzidine |
| **TNF-α** | Tumor necrosis factor-α |
| **Treg** | Regulatory T cell |
| **U** | Unit |
| **VCAM-1** | Vascular cell adhesion molecule-1 |
| **WBC** | White blood cell |
| **x** | Times |
| **ZAP-70** | Zeta-chain-associated protein kinase 70 |

# 1. Introduction

## 1.1 Cardiovascular disease

Cardiovascular diseases (CVDs) are the leading global cause of morbidity and mortality. According to the World Health Organization, about 18 million deaths, accounting for 32% of global deaths, were caused by CVDs in 2019[1].

CVDs comprise a number of disorders affecting the vasculature of heart and brain and manifest mainly as acute coronary syndrome (ACS), myocardial infarction (MI) or ischemic stroke (large artery atherosclerotic stroke, LAAS)[1,2].

The pathology of the disease has been linked to numerous co-existing conditions including elevated blood pressure, type 2 diabetes, or metabolic syndrome. Additionally, these co-morbidities are exacerbated by lifestyle-related risk factors such as unhealthy diet, physical inactivity, or nicotine abuse. As incidence risk steadily increases with age, CVDs have become a major issue in an aging society[3].

## 1.2 Atherosclerosis

Atherosclerosis is a persistent inflammatory condition affecting the medium and large arteries of the vascular system and is the main cause of CVDs. Immune responses originating from both arms of the immune system contribute to the deposition and development of lipid-rich lesions in the arterial wall resulting in thrombotic occlusion and unfavorable clinical results such as ACS, MI or LAAS[2,4,5].

### 1.2.1 Disease initiation

Atherosclerosis is initiated by endothelial dysfunction with enhanced permeability for lipids like low-density lipoprotein (LDL) cholesterol. After infiltrating the most internal layer of the blood vessel, known as the tunica intima, they are oxidized by reactive oxygen species and turn into oxidized LDL (oxLDL)[2,5].

Endothelial dysfunction is also accompanied by abundant adhesion of leucocytes, mainly monocytes and T cells, by attaching to adhesion molecules such as VCAM-1. The expression of these molecules can be further upregulated by oxLDL particles via nuclear factor-κB (Nf-κB) pathway involving cytokines like IL-1ß or TNF-α. After attachment, leucocytes migrate into the intima by diapedesis. This process is orchestrated not only by increased expression of selectins and adhesion molecules on the activated endothelium but also by endothelial-immobilized chemoattractants such as MCP-1 signalling through its receptor CCR2 and integrins presented by the invading inflammatory cells[4,5].

Once in the intima, monocytes undergo activation by macrophage colony-stimulating factor (M-CSF). They internalize oxLDL and lipids through scavenger receptor A and CD36 and differentiate into lipid-rich macrophages, so called foam cells. The involvement

of scavenger receptors for oxLDL, which are multifunctional pattern recognition receptors (PRRs), indicate a significant contribution of innate immune mechanisms in the process of atherogenesis. In addition, monocytes and activated T cells emit a variety of pro-inflammatory cytokines and growth factors promoting further immune cell recruitment[2,5].

Early lesions, which are mainly build of foam cells, LDL cholesterol and T cells, are referred to as fatty streaks[4].

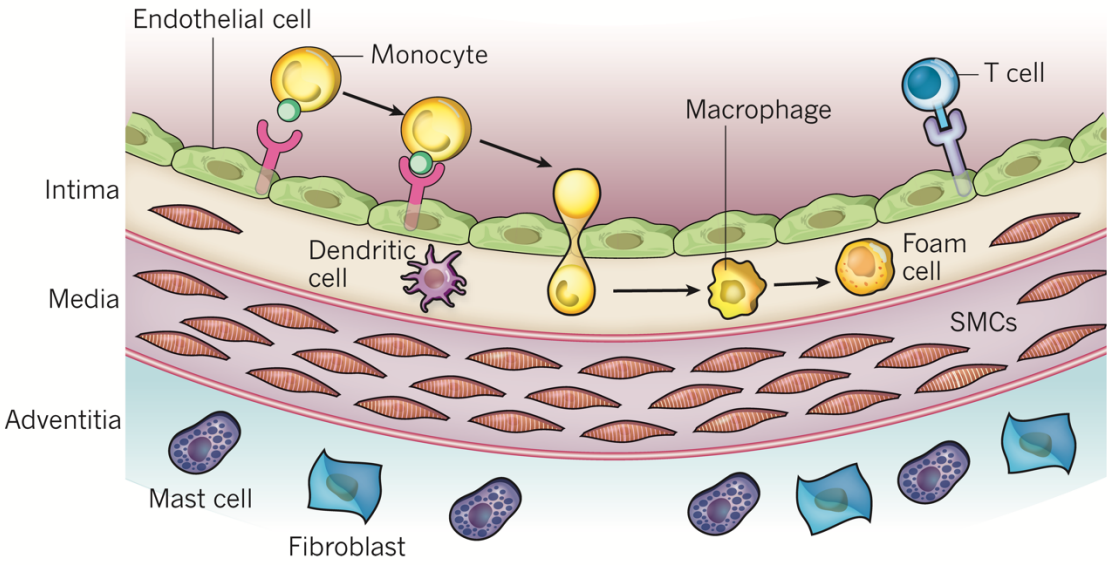


**Figure 1: Disease initiation.** A healthy blood vessel consists of three layers (from inside to outside): the intima, which is covered by endothelial cells, the media and the adventitia. Atherosclerosis is initiated by adhesion of blood leukocytes to the activated endothelium. After directed migration into the intima, monocytes transform into macrophages and, by uptake of lipids, into foam cells. Figure adapted with permission from Libby *et al.*, *Nature*, 2011[6].

### 1.2.2 Disease development and clinical complications

With disease development, the arterial wall is remodeled. An atherosclerotic plaque develops with the presence of inflammatory cells like monocytes/macrophages/foam cells, T cells, neutrophils, mast cells and dendritic cells (DCs) as well as lipids and apoptotic bodies building the necrotic center. A fibrous cap that covers and stabilizes the plaque core is formed by migrating and replicating smooth muscle cells (SMCs) and collagen[5].

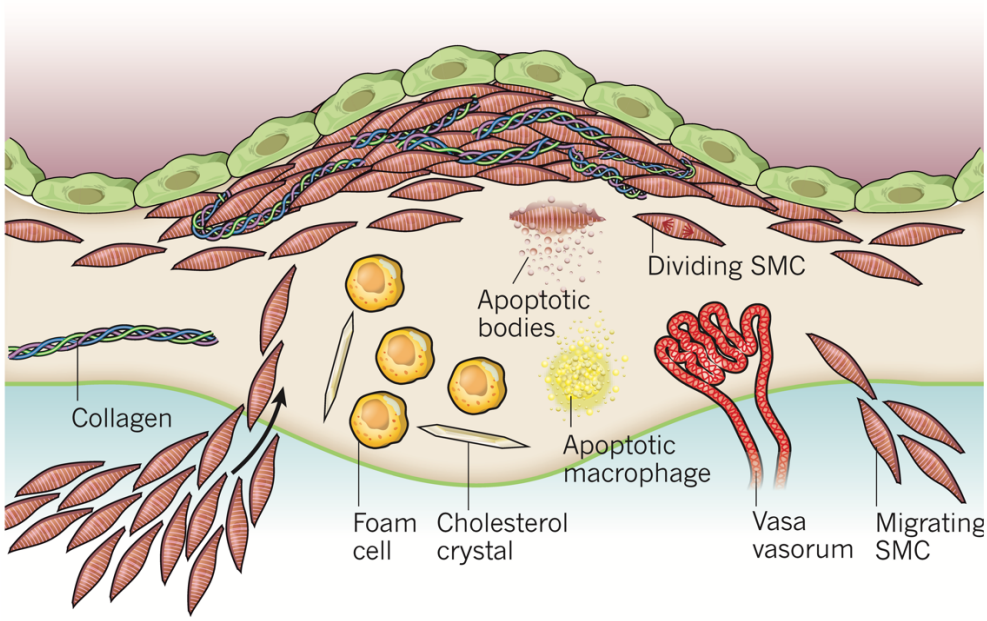


**Figure 2: Disease development.** Advanced atherosclerotic lesions are characterized by lipids and apoptotic bodies building a necrotic center. The migration of SMCs towards the intima and progressive synthesis of collagen lead to the formation of a fibrous layer that borders the necrotic center. Neovascularization is also typical at this stage. Figure with permission from Libby *et al.*, *Nature*, 2011[6].

The durability of the plaque is dependent on the extension and constitution of the fibrous cap on one hand and on the volume of the necrotic center on the other hand. With increasing replacement of SMCs and collagen by matrix metalloproteinases (MMPs), expressed by macrophages and mast cells, the plaque gets more vulnerable and prone to disrupt[4,7].

Plaque rupture can lead to thrombus formation resulting in narrowing or occlusion of the arterial lumen and limiting blood flow. In this way, depending on the location of the thrombotic occlusion, atherosclerosis may get clinically apparent as ACS, MI or LAAS[2,4,5].

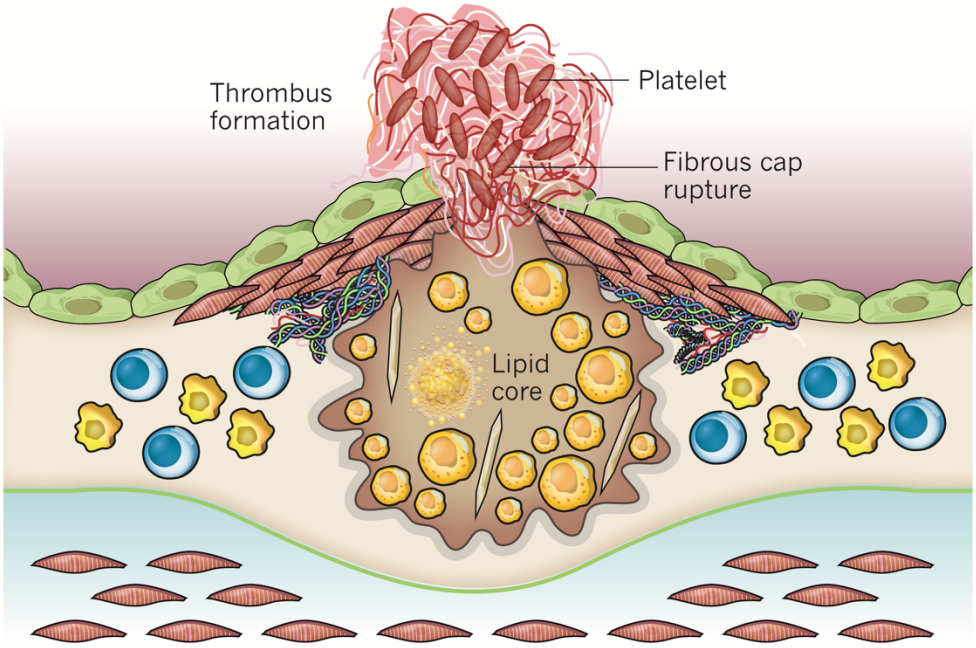


**Figure 3: Plaque rupture.** Thinning of the fibrous cap can result in plaque rupture triggering the coagulation system and thrombus formation. The extending thrombus may occlude the arterial lumen and clinically manifest in heart attacks or stroke. Figure with permission from Libby *et al.*, *Nature*, 2011[6].

### 1.2.3 Immune cells in atherosclerotic plaques

Various types of immune cells are present in atherosclerotic plaques, comprising primarily macrophages, T cells, mast cells and DCs[5].

Lesional macrophages were historically divided into pro-inflammatory and anti-inflammatory/reparative macrophages. While the latter, also termed M2 macrophages, are considered anti-atherogenic, the former, also termed M1 macrophages, produce inflammatory cytokines like TNF-α and are predominant in mature plaques[8].

Among T cell subgroups, CD4+ type-1 T-helper (Th) cells are the major player in inflammation and atherogenesis involving IFN-γ and TNF-α. Further T cell populations are anti-atherogenic regulatory T cells (Tregs), Th cell subpopulations like Th2 cells and cytotoxic CD8+ T cells. The latter are discussed in the context of plaque vulnerability[9].

Mast cells might, besides digesting surrounding matrix elements and secreting TNF-α, also contribute to plaque rupture[5,10].

DCs are antigen-presenting cells. By displaying a complex on the cell surface, formed by an antigenic peptide attached to a MHC protein, to T cells, they can initiate immune responses to plaque antigens[5].

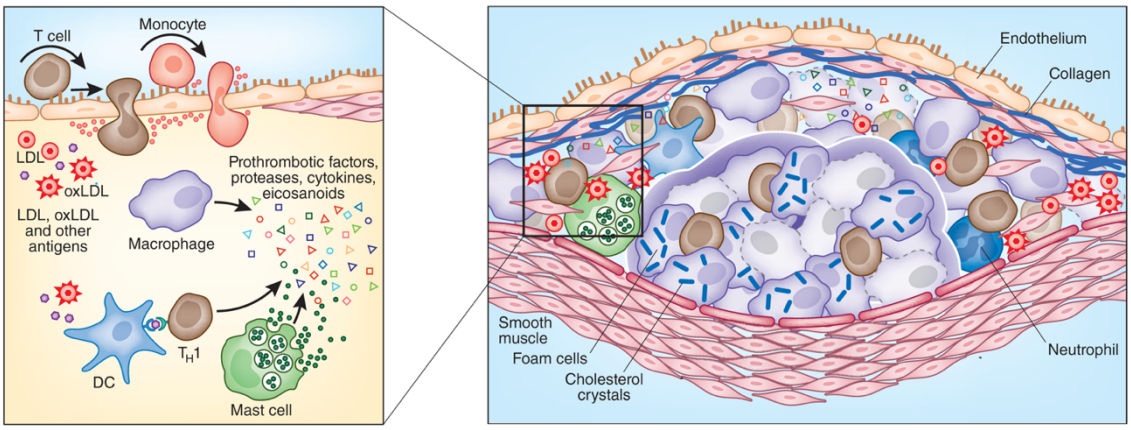


**Figure 4: Immune cells in atherosclerotic plaques.** Different types of cells comprising monocytes/ macrophages, T cells, mast cells and DCs are present throughout the plaque. Plasma lipoproteins like oxLDL can be found in the subendothelial region, while lipids, cholesterol crystals, and dying foam cells accumulate in the center of the plaque. Figure adapted with permission from Hansson and Hermansson, *Nat Immunol*, 2011[5].

## 1.3 B lymphocytes in atherosclerosis

### 1.3.1 B cell function and antibody structure

B cells have a central function in the humoral immune system as they produce antibodies. Antibodies, also known as immunoglobulins (Igs), can serve as B cell receptors (BCRs) on the B cell membrane or are secreted by plasma cells, the B cell progeny, into the extracellular space to protect against various pathogens[11].

They consist of two equal heavy (H-) and two equal light (L-) peptide chains with variable *N*-terminal regions. One variable region from each H-chain and L-chain ($V_H$ and $V_L$) make up the antigen-binding site, also referred to as antigen-binding fragment (Fab), laying down antibody specificity[11].

The diverse repertoire of antibody expressing B cells derives from the rearrangement of immunoglobulin gene segments in the course of B cell maturation and enables the detection of about $5x10^{13}$ different antigens[12].

Besides the variable domains at the *N*-terminus, all chains contain constant domains ($C_H$ and $C_L$). The H-chain domains $CH_2$ and $CH_3$ build the so-called crystallizable fragment (Fc) interacting with matching Fc receptors on effector cells and determining the Ig isotype (IgG, IgM, IgA, IgD or IgE). Signaling through Fc receptors can notably activate immune cells or induce the complement system[11].

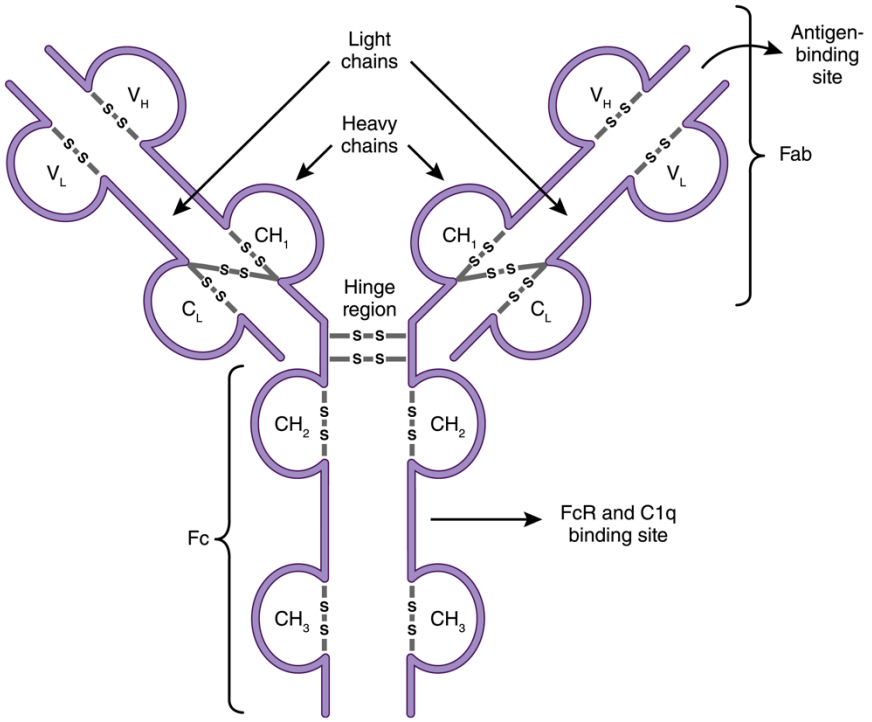


**Figure 5: Scheme of an antibody structure.** Their variable regions of the heavy and light chains ($V_H$ and $V_L$, respectively) build the specific antigen-binding fragment (Fab). The constant domains $CH_2$ and $CH_3$ of the heavy chains constitute the Fc region interacting with Fc receptors on effector cells or with the complement component C1q. Figure with permission from Hoffman *et al*., *Clin J Am Sec Nephrol*, 2016[11].

### 1.3.2 B cell subsets

Monocytes/macrophages and T cells and their involvement in the inflammatory atherogenic process have been described extensively so far. In recent times, also B cells have emerged as participants in atherogenesis. But the findings have been controversial as B cells have been shown to both, attenuate or exacerbate the development of atherosclerosis in mouse models indicating subtype-dependent effects of B cells[13-16].

Indeed, two major subsets, B1 and B2 cells, have been described[17]. B2 B cells dwell primarily in the spleen and comprise follicular (FO) B cells, which make up about 80% of splenic B cells, and marginal zone (MZ) B cells. Conventional FO B cells circulate within the blood stream and settle in splenic follicles. They are part of the adaptive immune system as they mature in secondary lymphoid organs (SLOs), including spleen, lymph nodes (LNs) and Peyer's Patches, in response to antigen-presenting T cells[11,17].

Upon germinal center (GC) reactions, involving isotype class switching and creation of high-affinity IgG, IgA or IgE antibodies, durable, high-affinity plasma cells and memory B cells are generated which provide an expedited immune response when the antigen is encountered again[18]. Additionally, there are short-lived plasmablasts in the circulation which are created extrafollicularly, missing affinity maturation, and therefore secreting low-affinity antibodies[18].

MZ B cells linger in the splenic marginal zone and belong to the innate immune system. They are able to defend against circulating blood-borne antigens that are filtering through

the spleen by producing natural IgM[11]. Besides, memory B cells displaying traits reminiscent of MZ B cells have been described in humans, which account for up to 40% of peripheral B cells[19].

B1 B cells represent only 5% of the total B cell population in the spleen, but inhabit serosal cavities, like the peritoneum and pleura, and contribute significantly to innate immunity. They provide immune responses against heterogenous antigens by producing low-affinity IgM antibodies[11,20]. B1 B cells can be further classified into B1a and B1b B cells and differ by the presence or absence of CD5 on their surface[17].

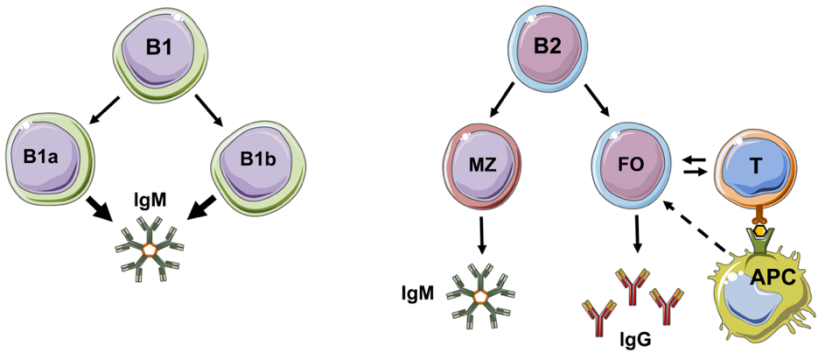


**Figure 6: Scheme showing B cell subsets.** B1 and B2 B cells. B1 B cells are subdivided into B1a and B1b B cells, each producing natural IgM. B2 B cells are subdivided into MZ B cells, which also produce IgM, and FO B cells, which mature in response to T cells and secrete high-affinity IgG, IgA or IgE. Figure adapted with permission from Srikakulapu and McNamara, *Am J Physiol Heart Circ Physiol*, 2017[17].

### 1.3.3 Early B cell development

B cell development originates in the bone marrow (BM) from hematopoietic stem cells (HSCs) and progresses through numerous maturation steps depending on the regulated expression of transcription factors such as Ebf1, Pax5 and PU.1[12,21,22].

HSCs differentiate into IL-7-producing lymphoid progenitors. Rearrangement of the Ig H-chain promoted by recombination-activating enzymes (Rag1/2) results in the creation and surface presentation of the pre-B cell receptor on pre-B cells. Additional reorganization of the Ig L-chain, along with the integration of the H-chain, forms the BCR of immature B cells. At this stage, self-reactive immature B cells with high-affinity autoreactive BCRs are eradicated through either receptor editing or clonal deletion via apoptosis. Only approximately 25% of the produced B cells pass this selection progress successfully and depart from the BM to undergo their ultimate maturation process in the spleen[12,22,23].

### 1.3.4 Final B cell development in SLOs

When leaving the BM and migrating into SLOs via blood stream, immature B cells undergo a transitional stage. In the spleen, two B cell subpopulations can been found: Type1 (T1) and Type2 (T2) transitional B cells[12,22]. T1 B cells pass a negative selection process regulated by constant BCR signals and BAFF survival signals to mature to the T2 stage[24]. BCR signals and further signaling pathways including Nf-κB and Bruton

tyrosine kinase (BTK) determine subsequent T2 B cell development. Potent BCR signals favor the maturation of FO B cells, while less potent signals mediate MZ B cell maturation. FO B cells can be categorized into FO1 B cells which necessitate BCR and BTK signaling for maturation and FO2 B cells which do not[11,25].

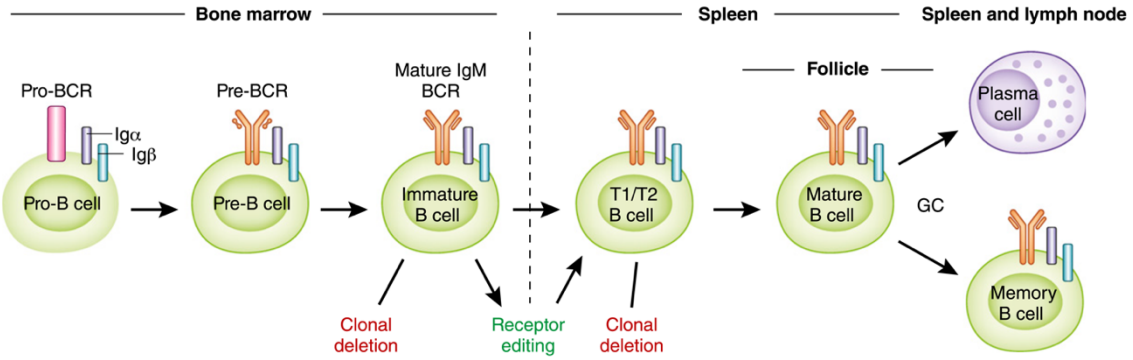


**Figure 7: B cell development.** The different stages in the BM and the spleen are indicated. Figure adapted with permission from Hoffman *et al.*, *Clin J Am Sec Nephrol*, 2016[11].

### 1.3.5 Humoral immune responses in atherosclerosis

Initially, B cells were regarded as protective players in atherosclerosis as shown in several studies including atherogenic mouse models. Enhanced lesion development was uncovered in splenectomized *Apoe-/-* mice as well as in *Ldlr-/-* mice after exposure to radiation and transplantation of B cell-deficient BM[14,15]. Later on, other studies demonstrated a marked reduction in plaque size after B cell suppression in *Apoe-/-* and *Ldlr-/-* mice, indicating pro-atherogenic effects of B cells[13,16]. Taken together, opposite behavior of the different B cell subsets is likely.

B1a B cells are considered to mediate atheroprotection by producing natural IgM antibodies[26]. IgM antibodies recognize and bind oxidation-specific epitopes (OSEs) on oxLDL and dying cells and thereupon inhibit oxLDL internalization and foam cell generation and regulate apoptotic cell clearance in the intima[27]. Similar effects have been observed for B1b B cells[28] as well as for MZ B cells[29]. Apart from producing natural IgM antibodies, MZ B cells can diminish T follicular helper response, again protecting against atherosclerosis[30]. Regulatory B cells (Bregs) exert their atheroprotective effects by secreting IL-10[31].

Opposingly, FO B cells are related to atheroprogression as they produce a variety of antibodies including IgG, IgA and IgE isotypes[27]. OxLDL specific IgG antibodies, as well as IgE antibodies, can activate macrophages and mast cells through their Fc receptors and thereby promote lesion formation[27]. IgG has also been associated with SMC proliferation and ensuing plaque vulnerability[32]. Nevertheless, the role of immunoglobulin classes, particularly IgG and IgA, remains elusive[27]. Besides, FO B cells impact CD4+ T cell transformation to IFN-γ-secreting Th1 cells and thus inflammation[13].

A more recent described population originating from peritoneal B1a B cells, the so called IRA B cells, produces granulocyte-macrophage colony-stimulating factor (GM-CSF)

which may be linked to DC activation and further Th1 cell generation during atherogenesis[33].

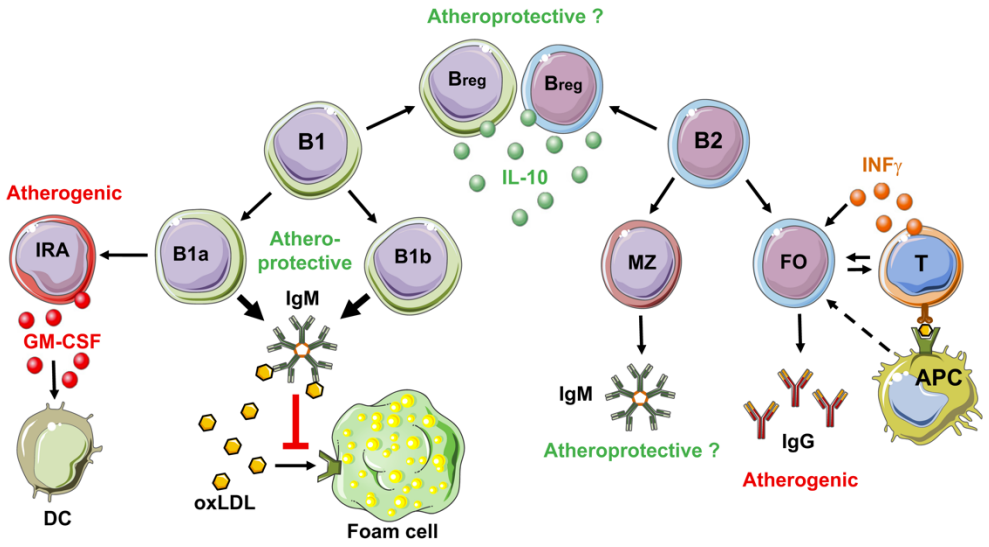


**Figure 8 (Completion of figure 6): B cell subsets and their immune responses in atherosclerosis.** B1a and B1b B cells are considered to be atheroprotective as they produce natural IgM that inhibits oxLDL uptake by macrophages and foam cell formation. Further potentially atheroprotective subsets are MZ B cells and IL-10-secreting Bregs. In contrast, atherogenic properties have been attributed to IRA B cells, which activate DCs through GM-CSF signaling, and FO B cells, which produce IgG and stimulate IFN-γ-secreting T cells. Figure adapted with permission from Srikakulapu and McNamara, *Am J Physiol Heart Circ Physiol*, 2017[17].

## 1.4 Artery tertiary lymphoid organs (ATLOs)

B cells appear in atherosclerotic lesions themselves but are more abundant in the tunica adventitia, the outermost tissue layer of the vessel, of brachiocephalic artery (BCA) and abdominal aorta (AA)[34,35].

In aged atherosclerosis-prone *Apoe-/-* mice, B lymphocytes have been detected within artery tertiary lymphoid organs (ATLOs)[36]. These are lymphoid aggregates which are located in the adventitia of BCA and AA, close to inflammation sites, and can be considered as centers of local humoral immunity. They vary from loosely arranged T and B cell aggregates to organized lymphoid tissues with distinct immune cell compartments, suggesting three consecutive stages of ATLO formation[37,38].

Stage I is defined by peri-adventitial T and B cell invasion via the vasa vasorum mediated by chemokines like CCL21 and CXCL13[38]. In stage II, lymphocytes form discrete T and B cell areas. Lymph vessels arise as well as lymph node- like conduits providing access to high endothelial venules (HEVs)[38]. Stage III is hallmarked by large T cell follicles, DCs, B cell follicles with ectopic GCs encompassing follicular dendritic cells (FDCs) and proliferating B cells as well as plasma cell niches in the periphery. Moreover, advanced ATLOs show increased lymph and blood vessel neogenesis and neoformation of HEVs[37,38].

The specific contribution of ATLOs to atherogenesis has not been determined so far. Nevertheless, B cells derived from ATLOs have been associated with atherogenesis-cushioning functions[39].

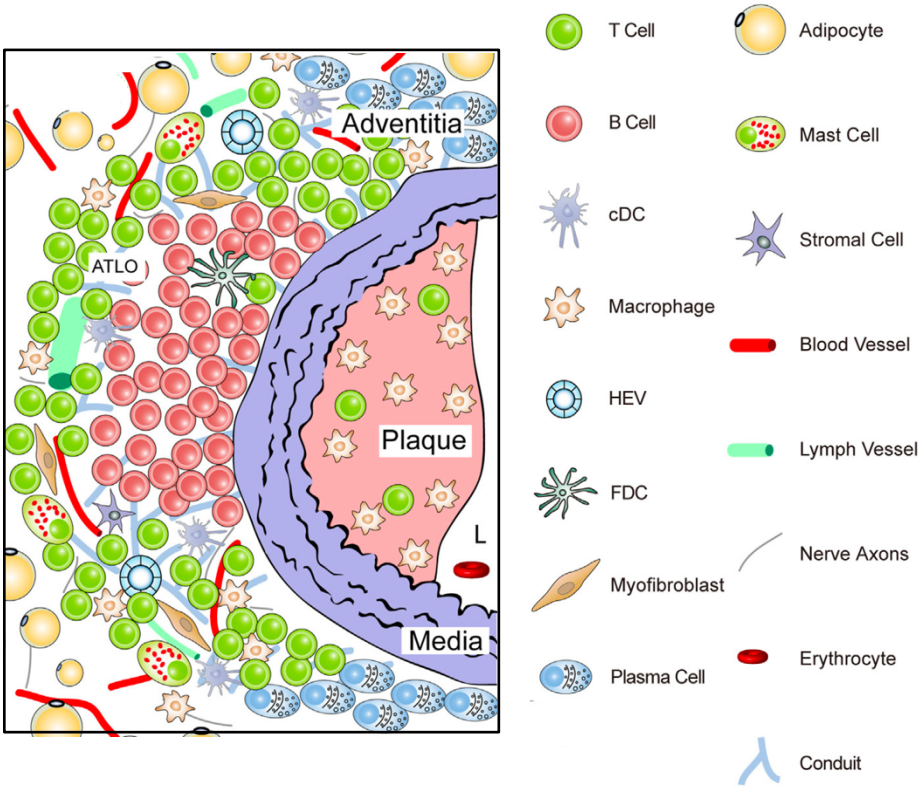


**Figure 9: Composition of ATLOs.** ATLOs are lymphoid aggregates in the adventitia of aged hyperlipidemic mice nearby atherosclerotic lesions. Advanced stages are characterized by structured T and B cell areas alongside plasma cell niches, several other immune cells, lymph and blood vessels and HEVs. Figure adapted with permission from Yin *et al.*, *Front Immunol*, 2016[38].

## 1.5 Chemokines in atherosclerosis

### 1.5.1 Structure and function of classical chemokines and their receptors

Chemokines have a fundamental role in inflammatory response and immunomodulation. They can be categorized into four major groups depending on their cysteine residues at the *N*-terminus, namely C-, CC-, CXC- and $CX_3C$- chemokines[40]. Chemokines, or chemotactic cytokines, can induce leukocyte trafficking. Some chemokines are constitutively expressed and secreted to regulate organ development and cell homeostasis. Others are only produced by cells upon inflammatory stimuli, though directing immune cells to the inflamed or injured site[41].

All chemokines show the same structural three-dimensional-fold, comprising the *N*-terminal loop, three ß-sheets and a *C*-terminal α-helix. They transmit signals by interacting with chemokine receptors, which are part of the GPCR superfamily[40]. Structural characteristics of chemokine receptors are still elusive. It has been assumed that all chemokine receptors share a *N*-domain on the cell surface, seven

transmembrane helices, three extracellular loops, three cytoplasmic loops and a cytoplasmic *C*-domain[42]. Receptors are named according to the binding chemokine subclass[40].

Binding of chemokines to their receptors involves dual binding sites, the chemokine *N*-terminal loop and the receptor *N*-domain on site one and chemokine *N*-terminal residues and receptor loops on site two. Both sites interact and adjust binding affinity and specificity to different extents[42]. Ligand/receptor engagement leads to the separation of the coupled G-protein trimer into subunits and subsequent activation of multiple signaling pathways[43].

The chemokine/chemokine receptor system exhibits a high degree of promiscuity as certain chemokines can bind to a number of chemokine receptors and, in turn, most chemokine receptors are shared by various chemokines of a specific subgroup. In contrast, some chemokines are restricted to a certain receptor[42].

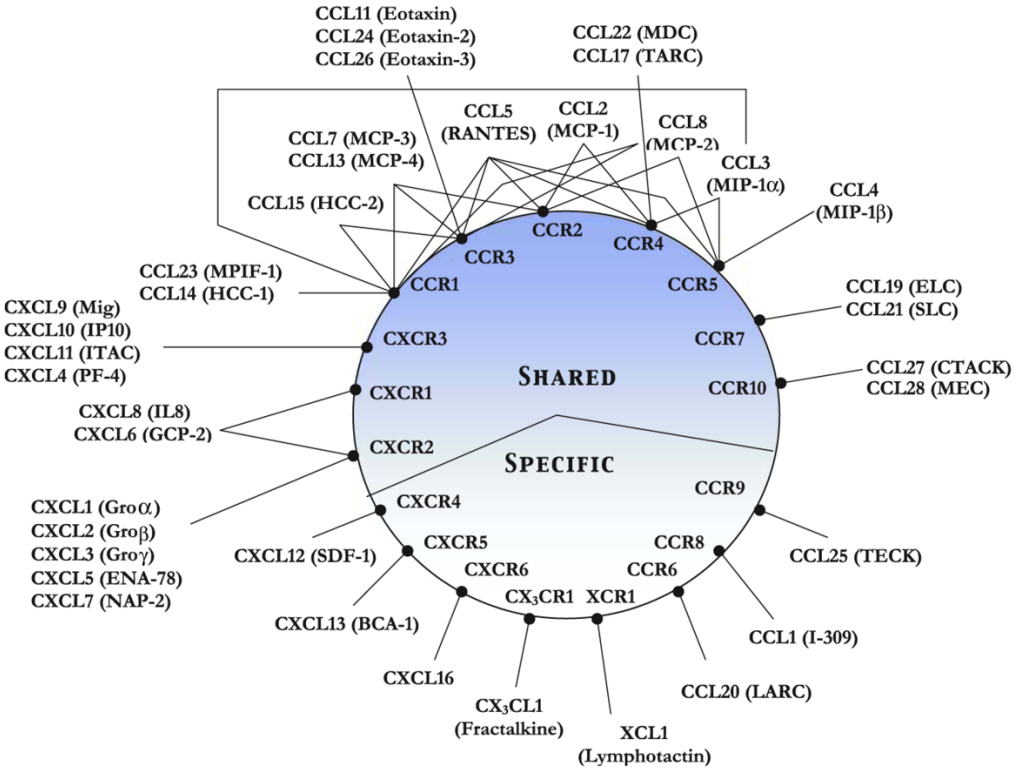


**Figure 10: Chemokine/chemokine receptor interactions.** Chemokines (outside the circle) and corresponding chemokine receptors (inside the circle) are depicted. Some chemokines can bind several receptors, and, in turn, some receptors are shared by various chemokines. Other interactions are specific. Figure with permission from Rajagopalan and Rajarathnam, *Biosci Rep*, 2006[42].

### 1.5.2 Chemokines in atherogenic cell recruitment

Chemokines play a pivotal role in atherogenesis as they induce the targeted movement of immune cells into atherosclerotic lesions. Though, chemokine ligand/receptor axes and their contribution to atherogenesis are complex and have been described controversially[44]. For instance, some chemokine receptors have been associated with monocyte recruitment (e.g. CCR2, CCR5, CX3CR1)[45] and infiltration into the lesion (e.g.

CCR1, CCR5)[46] or neutrophil recruitment (e.g. CCR1, CCR2, CCR5, CXCR2)[47] indicating pro-atherogenic functions of chemokines. Thus, there are ligand/receptor axes that are considered to be mainly atheroprotective (e.g. CXCL12/CXCR4)[48].

### 1.5.3 Atypical chemokines

Atypical chemokines (ACKs) have emerged as crucial drivers of atherogenesis as well. They show structural differences to classical chemokines as they lack the classifying canonical cysteine motif at the *N*-terminal end and do not have a chemokine-fold.[49]

ACKs serve as binding partners for classical chemokine receptors in a non-cognate manner and, in addition, as *bona fide* intracellular effectors. As they interact with classical chemokine receptors with high affinity and further induce chemotactic cell migration, they are also known as chemokine-like function cytokines. Prototypical examples of this protein class are alarmins, like HMGB1, or MIF[49].

## 1.6 Macrophage migration inhibitory factor (MIF)

### 1.6.1 Structural and functional aspects

MIF is a highly conserved cytokine with pleiotropic and inflammatory properties and is categorized as an ACK[50]. It was originally identified as a soluble factor released by lymphocytes inhibiting macrophage migration in delayed-type hypersensitivity. Therefore it has been referred to as ‘macrophage migration inhibitory factor’[51].

Mouse and human MIF proteins are about 90% identical over 115 amino acids[50]. X-ray crystallography and cross-linking analysis have revealed that MIF co-exists as monomers, dimers and trimers in solution, still elusive which oligomerization state is physiological[52,53]. The monomeric form of MIF is composed of two α-helices oriented in opposite directions, a ß-sheet with four strands and two extra ß-sheets participating in the process of oligomerization. Important characteristic elements are the *N*-like loop and the pseudo-(E)LR motif[54].

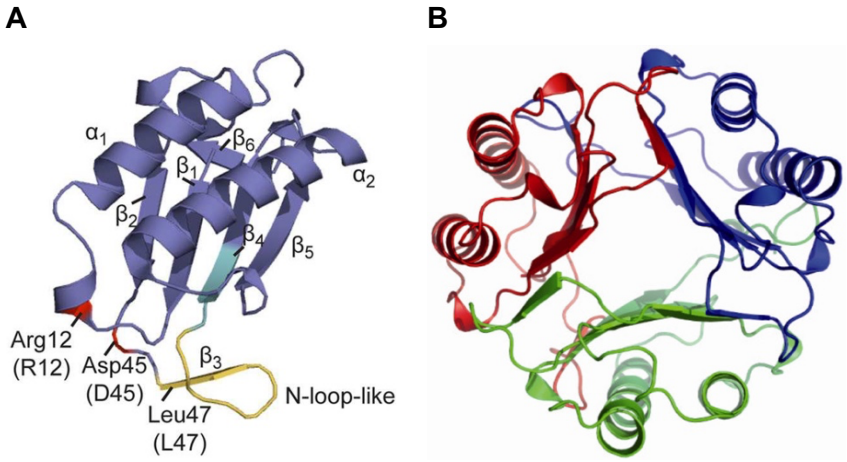


**Figure 11: Three-dimensional structure of MIF. A)** The monomeric form of MIF is composed of two α-helices oriented in opposite directions, a ß-sheet with four strands and two extra ß-sheets. Characteristic elements are the *N*-like loop (yellow), the pseudo-(E)LR motif (red) and the CALC motif (light blue) making up the catalytic center. Figure with permission from Tillmann et al., *Front Immunol*, 2013[55]. **B)** The trimeric form of MIF is composed of three monomers (each highlighted by a different color). Figure with permission from Merk *et al*., *Cytokine*, 2012[56].

MIF expression occurs broadly but mainly in immune cells like monocytes and T cells, endothelial cells (ECs), SMCs and thrombocytes, and is induced in response to several inflammatory stimuli including inflammatory cytokines, lipopolysaccharide (LPS) and oxLDL[57-59]. Unlike classical chemokines, MIF is consistently produced, deposited in intracellular reservoirs and secreted by a non-conventional pathway independent from a *N*-terminal leader sequence but including an ATP-binding cassette transporter[60,61].

MIF signals through different receptors including CXCR2, CXCR4, CXCR7 and CD74[62]. Its cognate receptor CD74 is referred to as MHC class II associated invariant chain[63]. MIF exerts chemotactic and arrest properties as it induces the release of chemokines, cytokines and adhesion molecules leading to accelerated cell enlistment. Through the engagement of CXCR2 and CXCR4, MIF mediates the recruitment of neutrophils, monocytes and T cells as well as the arrest of monocytes and T cells on the EC surface. Monocyte recruitment is also influenced by MIF binding to CD74/CXCR2 complexes[55,64]. Further pro-inflammatory effects have been investigated and involve several signaling pathways. For instance, MIF activates the JNK-MAPK cascade via CD74/CXCR4 pathway resulting in the expression of the inflammatory chemokine CXCL8 (IL-8)[65]. In turn, CXCL8 is involved in angiogenesis during inflammation[66]. Next, MIF affects cell survival and proliferation as binding to CD74 in complex with CD44 initiates signaling pathways involving ERK-MAPK and PI3K/AKT[67,68]. Moreover, MIF has shown enzymatic activity as a tautomerase as well as an oxidoreductase, yet uncertain which one is physiologically significant[61].

D-dopachrome tautomerase (D-DT), also known as MIF-2, is a structurally homologous molecule to MIF sharing tautomerase activity but missing structural features like the pseudo-(E)LR motif. So far, only CD74, but none of the classical chemokine receptors, has been verified to interact with D-DT[69].

### 1.6.2 MIF in atherosclerosis and cardiovascular disease

Upon its pro-inflammatory capacity, MIF has been associated with the pathogenesis of different inflammatory disorders including sepsis, autoimmunity and atherosclerosis[64,70,71]. It is upregulated in atherosclerotic lesions in humans and may be linked to coronary artery disease (CAD) as CAD patients have displayed elevated MIF levels in the circulation[72,73].

MIF amplifies lesional inflammation as demonstrated in experimental atherosclerosis studies utilizing *Mif* knockout in *Ldlr-/-* mice[74] or antibody neutralization in *Apoe-/-* mice on a high-fat diet (HFD)[75].

Different mechanisms supporting disease progression have been revealed. The pro-atherogenic effects of MIF are mainly due to the recruitment of immune cells into developing plaques through the engagement of CXCR2 and CXCR4[64]. In addition, MIF triggers the expression of several cytokines like TNF-α or IL-1ß[57]. Besides, MIF promotes oxLDL uptake by macrophages and thereby foam cell formation and plaque amplification as well as the upregulation of MMPs leading to increased plaque vulnerability[76,77].

In contrast, MIF signaling through CD74/CD44 promotes cardioprotection during myocardial ischemia via AMP-activating protein kinase (AMPK)[78].

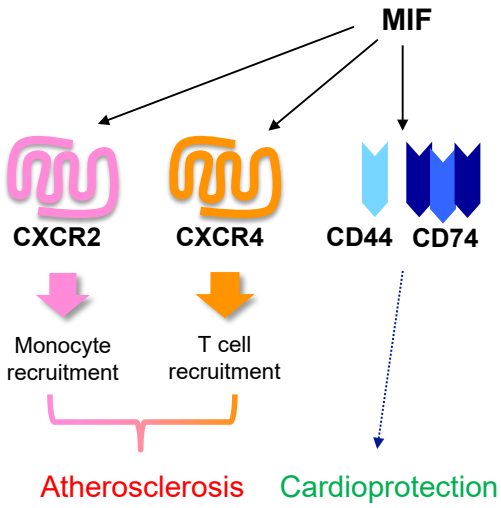


**Figure 12: MIF and its receptors in atherosclerosis – a simplified view.** MIF engaging with chemokine receptors mediates the recruitment of monocytes and T cells into developing atherosclerotic lesions and thereby atheroprogression. In contrast, MIF promotes cardioprotection by signaling through CD74/CD44.

### 1.6.3 Connection between MIF and B cells

A connection between MIF and B cell function seems natural as the B cell surface displays abundant expression of the MIF receptors CD74 and CXCR4[79]. Indeed, MIF engaging with CD74/CXCR4 has been implicated in B cell chemotaxis via a ZAP-70 signaling pathway[79]. Moreover, CD74 signaling induces transcriptional cascades including the transcription factor Nf-κB p65/RelA and its coactivator TAFII105, thereby supporting maturation and survival of mature B cells[80]. In the context of MIF, similar effects have been observed upon MIF signaling through CD74/CD44[68]. Pro-inflammatory

stressors, like LPS or TNF-α, have shown to stimulate CD74 expression in B cells and thus B cell proliferation, suggesting a MIF-induced B cell involvement in inflammatory processes[81]. For instance, the MIF/CD74 pathway in B cells has been linked to the development of systemic lupus erythematosus (SLE), an inflammatory autoimmune disease[82]. More recently, MIF signaling through CXCR7 has been related with B cell recruitment as well as receptor internalization[83].

Whereas MIF has been attributed to several B-cell-related autoimmune disorders, such as SLE or multiple sclerosis (MS), the role of MIF and B lymphocytes in atherosclerosis is still elusive[82,84].

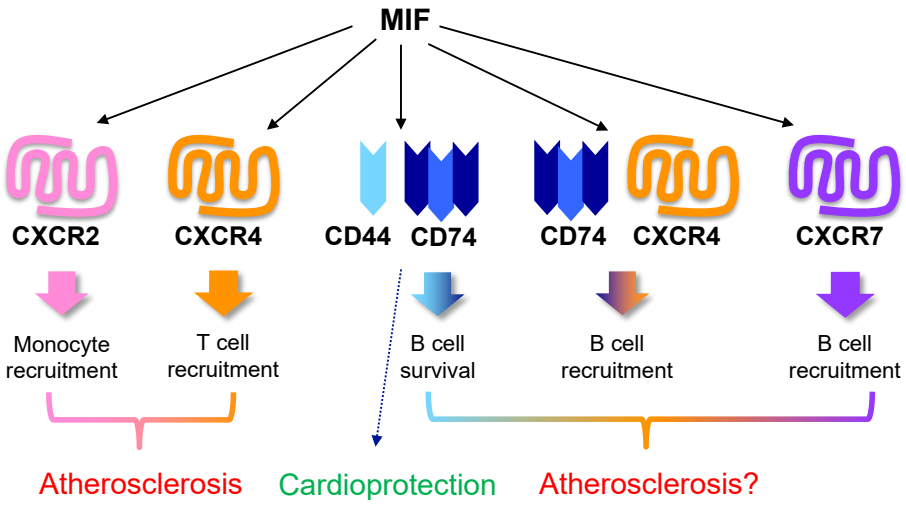


**Figure 13 (Completion of Figure 12): MIF, MIF receptors and B cells in atherosclerosis.** Binding of MIF to CD74/CD44 promotes B cell survival, whereas binding to CD74/CXCR4 or CXCR7 mediates B cell recruitment. The role of these signaling axes in atherosclerosis is still elusive.

Recent studies have conducted a more detailed analysis of *Mif* knockout within an *Apoe-/-* background, uncovering an association between MIF and B lymphocyte autoreactivity in the context of atherosclerosis featuring site-specific protection after an extended hyperlipidemic diet with lesion reduction specifically in the BCA and the AA. Besides, there have been indications that adventitial B cells are re-distributed into cluster-like formations in *Mif*-deficient compared to *Mif*-proficient *Apoe-/-* mice. Concomitantly, an altered B lymphocyte phenotype involving an atheroprotective autoantibody pattern has been observed upon *Mif*-deficiency[85]. Nevertheless, the cellular composition of these clusters has not been explored.

## 1.7 Aim of the study

CVDs have become a major issue in recent years, primarily due to an aging society. Atherosclerosis as the main underlying cause has been extensively studied. However, an enhanced understanding of the inflammatory pathways in atherogenesis, in particular over the course of aging, can yield substantial benefits for the development of treatment strategies.

MIF has been associated with inflammatory conditions including atherosclerosis. In recent times, B cells have emerged as crucial drivers in atherogenesis with subtype-dependent effects. While only a few B cells appear in atherosclerotic plaques, the majority accumulates in the adventitia of BCA and AA. In highly aged hyperlipidemic *Apoe-/-* mice, B cells have been detected in ATLOs contributing to local humoral immunity.

Recent studies have unveiled a heightened development of B cell-rich clusters in *Mif*-deficient *Apoe-/-* mice following 24 weeks of a HFD compared to age-matched *Apoe-/-* mice. Nevertheless, the constitution of these clusters has remained unclear, as well as links between B cells and MIF in atherogenesis in the context of aging. Indeed, a maximum of 14-26 weeks of HFD has been applied to atherogenic mouse models.

Based on this background, I planned to examine the effect of global *Mif*-deficiency on pro-atherogenic *Apoe-/-* mice throughout various stages of aging and HFD. Wildtype *Apoe-/-* mice were compared to *Apoe-/- Mif-/-* mice after 18, 30, 42 and 48 weeks of age, corresponding to 12, 24, 36 and 42 weeks of HFD, respectively.

I aimed to clarify how the previously described vascular region-specific atheroprotective phenotype in *Mif*-deficient *Apoe-/-* mice, with lesion reduction specifically in the BCA and the AA, develops during aging. Phenotypic lesion analyses were supplemented by fluorescence-activated cell sorting (FACS)-based immune cell profiling of blood and several organs.

Besides, my objective was to further resolve the role of B cells by analysis of peri-adventitial B cell clusters, encompassing immunostainings for ATLO-classifying structures including B cells, T cells, lymph vessels, HEVs and FDCs, as well as by delineation of atheroprotective versus atheroprogressive anti-oxLDL antibody profiles.

# 2. Materials

## 2.1 General laboratory equipment

**Table 1: List of general laboratory equipment**

| Equipment | Manufacturer |
|---|---|
| accuSpin™ Micro 17 Microcentrifuge | ThermoFisher Scientific, Dreieich, Germany |
| Analytical Balance MS | Mettler-Toledo GmbH, Gießen, Germany |
| BD FACSVerse™ flow cytometer | BD Biosciences, Heidelberg, Germany |
| BRAND™ accu-jet™ pro Pipet Controller | ThermoFisher Scientific, Dreieich, Germany |
| BRAND™ Transferpette™ S-8 | “ |
| Cryogenic Storage Chest Freezer | “ |
| Dmi8 fluorescent microscope | Leica Microsystems, Wetzlar, Germany |
| EnSpire™ Multimode Plate Reader | PerkinElmer, Hamburg, Germany |
| FiveEasy pH meter | Mettler-Toledo GmbH, Gießen, Germany |
| Fresco™ 17 Microcentrifuge | ThermoFisher Scientific, Dreieich, Germany |
| Gilson™ Pipetman™ Pipets (2/10/20/100/200/1000 µl) | “ |
| HERAfreeze™ HFU T Series -86°C Ultra-Low Temperature Freezer | “ |
| Hotplate | Bartscher GmbH, Salzkotten, Germany |
| HSC Heating Magnetic Stirrer | VELP Scientifica Srl, Usmate, Italy |
| Leica CM1950 Cryostat | Leica Microsystems, Wetzlar, Germany |
| Megafuge™ 16R | ThermoFisher Scientific, Dreieich, Germany |
| Microcentrifuge 5424 | Eppendorf SE, Hamburg, Germany |
| PCB precision balance | Kern & Sohn GmbH, Balingen, Germany |
| Refrigerator CP 3523 | Liebherr-Hausgeräte GmbH, Ochsenhausen, Germany |
| Scil Vet abc Plus+ blood analyzer | Scil Animal Care Company GmbH, Viernheim, Germany |

## 2.2 General consumables

**Table 2: List of general consumables**

| Consumable | Manufacturer |
|---|---|
| Corning® cell strainer (40 µm) | Sigma Aldrich/ Merck, Darmstadt, Germany |
| FACS tubes | BD Biosciences, Heidelberg, Germany |
| Falcon™ conical centrifuge tubes (15/50 ml) | ThermoFisher Scientific, Dreieich, Germany |

| | |
|---|---|
| Filter tips Biosphere® plus (2.5/10/200/1000 µl) | Sarstedt AG, Nürnbrecht, Germany |
| Micro sample tubes K3 EDTA (1.3 ml) | ” |
| Mr. Frosty™ freezing container | ThermoFisher Scientific, Dreieich, Germany |
| Nalgene™ cryo tubes | ” |
| Needles (20/23/27 G) | B. Braun SE, Melsungen, Germany |
| Nunc MaxiSorp™ 96-well plates | ThermoFisher Scientific, Dreieich, Germany |
| Pipet tips Biosphere® plus (20/200/1000 µl) | Sarstedt AG, Nübrecht, Germany |
| Reaction tubes (0.5/1.5/2 ml) | Carl Roth, Karlsruhe, Germany |
| SERAFLEX® sutures (USP 7/0) | Serag-Wiessner GmbH, Naila, Germany |
| Serological pipets (5/10/25 ml) | Greiner Bio-One GmbH, Frickenhausen, Germany |
| SuperFrost® Plus microscope slides | ThermoFisher Scientific, Dreieich, Germany |
| Syringes (1/2/5/10/20 ml) | B. Braun SE, Melsungen, Germany |

## 2.3 Chemicals and reagents

**Table 3: List of chemicals and reagents**

| Chemical/ reagent | Manufacturer |
|---|---|
| Acetone | Sigma Aldrich/ Merck, Darmstadt, Germany |
| BD FACSuite™ CS&T Research Beads | BD Biosciences, Heidelberg, Germany |
| Bovine serum albumin (BSA) | Carl Roth, Karlsruhe, Germany |
| DAPI (4’,6-Diamidino-2-phenylindole) | Sigma Aldrich/ Merck, Darmstadt, Germany |
| Domitor® (Medetomidine) 1 mg/ml | Pfizer GmbH, Berlin, Germany |
| Donkey serum | Sigma Aldrich/ Merck, Darmstadt, Germany |
| Eosin G solution | “ |
| Ethanol | “ |
| Ethylenediaminetetraacetic acid (EDTA) | “ |
| Fentanyl-Janssen® (Fentanyl) 0.05 mg/ml | Janssen-Cilag GmbH, Neuss, Germany |
| Fluoromount™ aqueous mounting medium | Sigma Aldrich/ Merck, Darmstadt, Germany |
| Goat serum | “ |
| Heparin sodium salt | Carl Roth, Karlsruhe, Germany |
| Isopropanol (2-Propanol) | Sigma Aldrich/ Merck, Darmstadt, Germany |
| Kaiser’s glycerin gelatin mounting media | Carl Roth, Karlsruhe, Germany |

| | |
|---|---|
| Low density lipoprotein from human plasma, oxidized (OxLDL) | ThermoFisher Scientific, Dreieich, Germany |
| Mayer's hematoxylin solution | Sigma Aldrich/ Merck, Darmstadt, Germany |
| Midazolam-ratiopharm® (Midazolam) 5 mg/ml | Ratiopharm GmbH, Ulm, Germany |
| Oil-Red-O (ORO) | Sigma Aldrich/ Merck, Darmstadt, Germany |
| Paraformaldehyde (PFA) | " |
| Phosphate-buffered saline (PBS) | ThermoFisher Scientific, Dreieich, Germany |
| Pierce™ 3,3',5,5'-tetramethylbenzidine (TMB) substrate solution | " |
| Propylene glycol (1,2-Propanediol) | Carl Roth, Karlsruhe, Germany |
| Red blood cell (RBC) lysis buffer | BioLegend, Koblenz, Germany |
| Sodium bicarbonate ($NaHCO_3$) | Carl Roth, Karlsruhe, Germany |
| Sodium carbonate ($Na_2CO_3$) | " |
| Sodium chloride (NaCl) | " |
| Sulfuric acid ($H_2SO_4$) | " |
| Tissue-Tek® O.C.T.™ compound | Sakura Finetek, Staufen, Germany |
| VECTASHIELD® antifade mounting medium | Vector Laboratories/ Biozol GmbH, Eching, Germany |
| Xylene | Sigma Aldrich/ Merck, Darmstadt, Germany |

## 2.4 Solutions and buffers

### 2.4.1 Solutions for animal treatment

**Table 4: List of solutions for animal treatment**

| Solution | Composition |
|---|---|
| Anesthesia | Medetomidine (0.5 mg/kg final)<br>Midazolam (5 mg/kg final)<br>Fentanyl (0.05 mg/kg final)<br>in 0.9% NaCl |
| Perfusion solution, pH 7.4 | 100 U/ml heparin<br>10 mM EDTA<br>in PBS |

### 2.4.2 Solutions and buffers for immunostaining and FACS

**Table 5: List of solutions and buffers for immunohistochemistry/immunofluorescence and flow cytometry**

| Solution/ buffer | Composition |
|---|---|
| Blocking solution, pH 7.4 | 5% donkey/goat serum<br>1% BSA<br>in PBS |
| FACS staining buffer, pH 7.4 | 0.5% BSA<br>in PBS |
| ORO solution for aortic root | 0.5% ORO<br>in propylene glycol |
| ORO solution for aorta | 0.5% ORO<br>in isopropanol |

### 2.4.3 Solutions and buffers for ELISAs

**Table 6: List of solutions and buffers for ELISAs**

| Solution/ buffer | Composition |
|---|---|
| Blocking solution | 2% BSA<br>in PBS |
| Carbonate buffer, pH 9.7 | 34.8 mM $NaHCO_3$<br>15 mM $Na_2CO_3$<br>in dd$H_2O$ |
| Stop solution | 0.5 M $H_2SO_4$<br>in dd$H_2O$ |

## 2.5 Antibodies

### 2.5.1 Antibodies for immunofluorescence stainings

**Table 7: List of antibodies for immunofluorescence stainings**

| Antibody | Conjugate | Cell target | Manufacturer |
|---|---|---|---|
| Rat anti-mouse CD45R/B220 | - | B cells | BD Biosciences, Heidelberg, Germany |
| Hamster anti-mouse CD3e | - | T cells | ” |
| Rat anti-mouse CD68 | - | Macrophages | Bio-Rad, Puchheim, Germany |
| Rat anti-mouse CD35 | - | FDCs | BD Biosciences, Heidelberg, Germany |

| | | | |
|---|---|---|---|
| Rabbit anti-mouse Lyve-1 | - | Lymph vessels | Acris Antibodies, Herford, Germany |
| Rat anti-mouse PNAd | - | HEVs | BD Biosciences, Heidelberg, Germany |
| Rat anti-mouse ER-TR7 | - | Reticular fibroblasts and fibres, connective tissue | Abcam, Berlin, Germany |
| Goat anti-mouse CXCL13 | - | Connective tissue cells | R&D Systems, Wiesbaden-Nordenstadt, Germany |
| Rabbit anti-mouse CollagenIV | - | Basement membrane | Bio-Rad, Puchheim, Germany |
| Goat anti-rat IgG | AF488 | - | ThermoFisher Scientific, Dreieich, Germany |
| Goat anti-hamster IgG | Cy3 | - | Jackson ImmunoResearch, Hamburg, Germany |
| Donkey anti-rabbit IgG | Cy3 | - | ” |
| Goat anti-rat IgM | Cy5 | - | ThermoFisher Scientific, Dreieich, Germany |
| Donkey anti-goat IgG | AF647 | - | “ |

### 2.5.2 Antibodies for flow cytometric analyses

**Table 8: List of antibodies for flow cytometric analyses**

| Antibody | Conjugate | Cell target | Manufacturer |
|---|---|---|---|
| Anti-mouse CD45 | APC-Cy7 | Leukocytes | BioLegend, Koblenz, Germany |
| Anti-mouse CD3e | FITC | T cells | Miltenyi Biotec, Bergisch Gladbach, Germany |
| Anti-mouse CD4 | PE | $CD4^+$ T cells | “ |
| Anti-mouse CD8a | PE-Cy7 | $CD8a^+$ T cells | ThermoFisher Scientific, Dreieich, Germany |
| Anti-mouse CD19 | PerCP-Cy5.5 | B cells | BioLegend, Koblenz, Germany |
| Anti-mouse CD19 | APC | B cells | “ |
| Anti-mouse CD43 | PE | B1a B cells/ B1b B cells | “ |

| | | | |
|---|---|---|---|
| Anti-mouse CD5 | FITC | B1a B cells | “ |
| Anti-mouse CD23 | PE-Cy7 | B2 B cells | ” |
| Anti-mouse CD11b | FITC | Monocytes/ neutrophils | Miltenyi Biotec, Bergisch Gladbach, Germany |
| Anti-mouse CD115 | PE | Monocytes | ThermoFisher Scientific, Dreieich, Germany |
| Anti-mouse Ly6G | PerCP-Cy5.5 | Neutrophils | “ |
| REA Control | FITC | - | Miltenyi Biotec, Bergisch Gladbach, Germany |
| Rat IgG2a,κ | FITC/ PE/ APC/ PerCP-Cy5.5/ PE-Cy7 | - | BioLegend, Koblenz, Germany |
| Rat IgG2b,κ | FITC/ PE/ PerCP-Cy5.5/ APC-Cy7 | - | “ |
| Rat IgM,κ | PE | - | ” |

### 2.5.3 Antibodies for ELISAs

**Table 9: List of antibodies for ELISAs**

| Antibody | Conjugate | Manufacturer |
|---|---|---|
| Goat anti-mouse IgG | HRP | Abcam, Berlin, Germany |
| Goat anti-mouse IgM | HRP | ThermoFisher Scientific, Dreieich, Germany |

## 2.6 Kits

**Table 10: List of commercial kits**

| Kit | Manufacturer |
|---|---|
| Cayman’s Cholesterol Fluorometric Assay kit | Cayman Chemicals/ Biomol GmbH, Hamburg, Germany |
| Cayman’s Triglyceride Calorimetric Assay kit | ” |

## 2.7 Mice

### 2.7.1 Mouse strains

**Table 11: List of mouse strains**

| Genotype | Mouse strain | Origin/ Reference |
|---|---|---|
| **Apoe-/-** | C57BL/6-J | Charles River Laboratories, Sulzfeld, Germany |
| **Apoe-/-** | C57BL/6-J | In house breeding at BernhagenLab |
| **Mif-/-** | C57BL/6-J | “[86] |
| **Apoe-/- Mif-/-** | C57BL/6-J | “[85] |

### 2.7.2 Mouse diets

**Table 12: List of mouse diets**

| Diet | Manufacturer |
|---|---|
| Regular chow diet | Ssniff Spezialdiäten GmbH, Soest, Germany |
| Western diet (0.21% cholesterol) | “ |

## 2.8 Software

**Table 13: List of software used for application and analysis**

| Software | Supplier |
|---|---|
| BD FACSuite™ | BD Biosciences, USA |
| FlowJo | Tree Star, USA |
| GraphPad Prism 9 | GraphPad Software Inc., USA |
| ImageJ | NIH, USA |

# 3. Methods

## 3.1 Mice

Atherosclerotic-prone C57BL/6 *Apoe-/-* mice and C57BL/6 *Apoe-/- Mif-/-* mice were housed and bred in a controlled and specific pathogen-free environment in the animal facility of the Center for Stroke and Dementia Research. To generate *Apoe-/- Mif-/-* mice, *Apoe-/-* mice were backcrossed with global *Mif* gene-deficient mice (*Mif-/-*), initially created by Dr. Fingerle-Rowson and Prof. Bucala[86], for at least 10 generations. All mouse experiments were approved by local authorities (approval ROB-55.2-2532.Vet_02-18-040) and were performed in accordance with the German animal protection law. Mice were sacrificed while under anesthesia with medetomidine, midazolam and fentanyl (MMF).

### 3.1.1 Western diet

Female mice were subjected to a regular chow diet until 6 weeks of age and for an additional 12, 24, 36 or 42 weeks to a 'Western-type' high-fat diet (HFD) containing 0.21% cholesterol and 21.2% total fat.

### 3.1.2 Isolation of tissues

After disinfection of the skin, blood was withdrawn by heart puncture and transferred into EDTA-containing tubes. Approximately 50 µl blood were used to determine hematologic parameters with the Scil Vet abc Plus+ blood analyzer. For plasma extraction, the remaining blood was centrifuged at 400 x g for 15 min at 4°C. The clear supernatant (plasma) was instantly frozen using liquid nitrogen and preserved at -79°C, the cell-containing pellet was maintained on ice for fluorescence-activated cell sorting (FACS) analysis.

The vascular system was flushed with 15 ml of perfusion solution (100 U/ml heparin, 10 mM EDTA in PBS, pH 7.4) followed by 15 ml of PBS. Spleen, LNs and BM of femur and tibia were isolated for FACS analysis.

To identify the BCA, the right subclavian and the right common carotid artery were exposed and bound off next to the bifurcation. The BCA as well as the aortic root were isolated, embedded in Tissue-Tek® O.C.T.™ compound and preserved at -79°C until preparation of cryosections.

The whole aorta, including all bed regions, was isolated, pinned onto a slide and subjected to overnight fixation in 1% PFA at 4°C. The following day, the aorta was removed from the surrounding adipose tissue and from the adventitial layer, opened lengthwise and pinned onto a slide with the endothelium facing upwards (*en face* preparation). The aorta was re-fixed in 4% PFA before Oil-Red-O (ORO) staining.

## 3.2 Lipid analysis

### 3.2.1 Cholesterol quantification

Plasma cholesterol levels were quantified using Cayman's Cholesterol Fluorometric Assay kit following the manufacturer's protocol. Plasma was diluted 1:2000 in cholesterol assay buffer and mixed 1:1 with assay cocktail (4.745 ml cholesterol assay buffer, 150 µl cholesterol detector, 50 µl cholesterol assay horseradish peroxidase (HRP) and 5 µl cholesterol esterase) in a 96-well plate. After incubation for 30 min at 37°C in the dark, the fluorescence was measured at an excitation wavelength of 535 nm and an emission wavelength of 590 nm by an EnSpire™ Multimode Plate Reader. Cholesterol levels were determined based on diluted cholesterol standards ranging from 2 to 20 µM.

### 3.2.2 Triglyceride quantification

Plasma triglyceride levels were quantified using Cayman's Triglyceride Calorimetric Assay kit following the manufacturer's protocol. Plasma was mixed 1:10 with a previously diluted enzyme cocktail in a 96-well plate and incubated for 15 min at room temperature (RT). The absorbance was measured at a wavelength of 450 nm by an EnSpire™ Multimode Plate Reader. Triglyceride levels were determined based on diluted triglyceride standards ranging from 3.125 to 200 mg/dl.

## 3.3 Atherosclerotic lesion assessment

### 3.3.1 ORO staining of aortic root

ORO staining was performed to quantify atherosclerotic lesion size in the aortic root and the aorta. First, 5 µm thick transverse cryosections of the aortic root were generated and attached to glass slides. The slides were air-dried for 5 min and then hydrated in PBS for 2 min. Plaques were stained with ORO solution (0.5% in propylene glycol) for 45 min at 37°C and, after flushing with water, nuclei were stained with Mayer's hematoxylin solution. The slides were again flushed with water, air-dried, and mounted with Kaiser's glycerin gelatin mounting media. Images were taken with the DMi8 microscope and lesion size quantified using ImageJ. For each mouse, mean values of 12 serial sections, spaced 50 µm apart, were calculated.

### 3.3.2 ORO (*en face*) staining of aorta

The aorta was stained in ORO solution (0.5% in isopropanol) for 30 min at RT and then washed in 60% isopropanol 10 times. The tissue was flushed with water and mounted with Kaiser's glycerin gelatin mounting media. Images were taken with the DMi8 microscope and lesion size quantified using FlowJo. The ORO-stained plaque area was depicted as percentage of the overall aortic surface.

### 3.3.3 H&E staining of brachiocephalic artery

Hematoxylin-Eosin (H&E) staining was conducted to quantify atherosclerotic lesion size in the BCA. For this, 5 µm thick transverse cryosections of the BCA were generated and attached to glass slides. The slides were air-dried for 30 min at RT and then hydrated in PBS for 2 min. Subsequently, nuclei were stained with hematoxylin solution for 15 min at RT. The slides were rinsed with water for 10 min, stained with Eosin G solution for 10 sec and dehydrated with 95% ethanol, 100% ethanol and xylene for 2 x 2 min each. The slides were air-dried and mounted with VECTASHIELD® antifade mounting medium. Images were taken with the DMi8 microscope and lesion size quantified using ImageJ. The plaque area was depicted as percentage of the overall inner vessel area. For each mouse, mean values of 12 serial sections, spaced 50 µm apart, were calculated.

### 3.3.4 Immunofluorescence of brachiocephalic artery

Immunohistochemistry was performed to detect different cells in the adventitia of the BCA. First, 5 µm thick transverse cryosections of the BCA were generated and attached to glass slides. The sections were fixed with acetone for 6 min at 4°C, air-dried for 30 min at RT and then rehydrated in PBS for 10 min. Next, the sections were treated with blocking solution (5% donkey/goat serum, 1% bovine serum albumin (BSA) in PBS, pH 7.4) for 30 min and incubated with the primary antibodies diluted in blocking solution overnight at 4°C. The primary antibodies are directed against cell-specific markers (**Table 14**). The following day, slides were washed in PBS and incubated with the respective fluorescently labeled and diluted secondary antibodies for 1 h at RT (**Table 15**). Nuclei were counterstained with DAPI. The slides were washed in PBS and mounted with Fluoromount$^{TM}$ aqueous mounting medium. Images were taken with the Dmi8 microscope and analyzed using ImageJ.

**Table 14: List of primary antibodies for immunofluorescence stainings**

| Cell type/ Structure | Marker | Primary antibody | Dilution |
|---|---|---|---|
| B cells | CD45R/B220 | Rat anti-mouse CD45R/B220 | 1:100 |
| T cells | CD3e | Hamster anti-mouse CD3e | ” |
| Macrophages | CD68 | Rat anti-mouse CD68 | ” |
| FDCs | CD35 | Rat anti-mouse CD35 | ” |
| Lymph vessels | Lyve-1 | Rabbit anti-mouse Lyve-1 | 1:500 |
| HEVs | PNAd | Rat anti-mouse PNAd | 1:50 |
| Reticular fibroblasts and fibers, connective tissue | ER-TR7 | Rat anti-mouse ER-TR7 | 1:500 |
| Connective tissue cells | CXCL13 | Goat anti-mouse CXCL13 | 1:25 |
| Basement membrane | Collagen IV | Rabbit anti-mouse Collagen IV | 1:500 |

**Table 15: List of secondary antibodies for immunofluorescence stainings**

| Secondary antibody | Conjugate | Dilution |
|---|---|---|
| Goat anti-rat IgG | AF488 | 1:500 |
| Goat anti-hamster IgG | Cy3 | 1:300 |
| Donkey anti-rabbit IgG | Cy3 | ” |
| Goat anti-rat IgM | Cy5 | ” |
| Donkey anti-goat IgG | AF647 | ” |

## 3.4 Flow cytometric analysis

Flow cytometry was performed to determine immune cell populations in blood, spleen, BM and LNs. Single cell suspensions were obtained from isolated spleen, BM and LNs by sieving the cells through a cell strainer. All suspensions including the beforehand obtained blood pellets underwent red blood cell (RBC) lysis using RBC lysis buffer, followed by washing in PBS.

Cells were stained with fluorescently labeled antibodies targeting cell type-specific surface markers (**Table 16**) for 30 min on ice in the dark. The antibodies were diluted 1:100 in FACS staining buffer (0.5% BSA in PBS, pH 7.4). Next, the cells were washed with FACS buffer and centrifuged for 5 min at 300 x g and 4°C. Directly thereafter, flow cytometric analysis was performed utilizing a BD FACSVerse$^{TM}$ instrument with a 3 laser, 8 color (4-2-2) configuration. Cells stained with respective isotype control antibodies were used as controls. FlowJo software was used for analysis and displayed as dot plots showing the distribution of the fluorescence signal at a logarithmic scale.

**Table 16: List of cell type-specific surface markers**

| Cell type | Surface markers |
|---|---|
| Leukocytes | $CD45^+$ |
| T cells | $CD45^+$ $CD3e^+$ |
| $CD4^+$ T cells | $CD45^+$ $CD3e^+$ $CD4^+$ |
| $CD8a^+$ T cells | $CD45^+$ $CD3e^+$ $CD8a^+$ |
| B cells | $CD45^+$ $CD19^+$ |
| B1a B cells | $CD45^+$ $CD19^+$ $CD43^+$ $CD23^-$ $CD5^+$ |
| B1b B cells | $CD45^+$ $CD19^+$ $CD43^+$ $CD23^-$ $CD5^-$ |
| B2 B cells | $CD45^+$ $CD19^+$ $CD43^-$ $CD23^+$ $CD5^-$ |
| Monocytes | $CD45^+$ $CD11b^+$ $CD115^+$ |
| Neutrophils | $CD45^+$ $CD11b^+$ $Ly6G^+$ |

## 3.5 Anti-oxLDL antibody ELISA

Plasma anti-oxLDL antibody levels were measured using a modified enzyme-linked immunosorbent assay (ELISA). Plates were coated with a diluted solution of 1 µg/ml oxLDL in carbonate buffer (34.8 mM $NaHCO_3$, 15 mM $Na_2CO_3$ in $ddH_2O$, pH 9.7) for 1 h

at 37°C. After washing the plates three times with 100 µl of blocking solution (2% BSA in PBS), they were blocked for 1 h at 37°C. 50 µl of plasma diluted 1:100 in blocking solution were applied , followed by incubation for 1 h at 37°C and thorough washing . Next, 50 µl of antibodies against IgG and IgM labeled with HRP and diluted 1:500 in blocking solution were added and incubated for 1 h at 37°C. After washing three times, 100 µl of Pierce™ TMB substrate solution were added for 5 min and the reaction was stopped by 50 µl of stop solution (0.5 M $H_2SO_4$ in $ddH_2O$). The absorbance was recorded at a wavelength of 450 nm by an EnSpire™ Multimode Plate Reader.

## 3.6 Statistics

All statistical analyses were performed by GraphPad Prism 9. Data were tested for normality with D'Agostino-Pearson test and analyzed by two-tailed Student's t-test (parametric) or Mann-Whitney test (non-parametric) as appropriate. To conduct multiple comparisons, two-way ANOVA with Sidak's multiple comparison was applied. $P<0.05$ was regarded as statistically significant.

# 4. Results

*A part of the results presented in the following section has already been published in the peer reviewed FASEB J publication by Krammer, Yang, Reichl et al., the corresponding bioRxiv preprint by Krammer, Yang, Reichl et al. and in the corresponding Appendix A: Publication III of C. Krammer's dissertation. I am a key contributing author on these publications. See the preface on page 6:* ***Published Manuscripts****.*

The results give insight into the connection between MIF and B lymphocytes in atherosclerotic pathology and unravel age-related effects.

## 4.1 Vascular region-specific atheroprotection owing to *Mif*-deficiency is lost in aged *Apoe-/-* mice

*In the following section, Table 17, 18 and 19 and Figure 14a and 14b have already been published in part in the peer reviewed FASEB J publication by Krammer, Yang, Reichl et al. 2023 and the corresponding preprints.*

MIF and its role in atherosclerosis has earlier been described in atherogenic *Apoe-/-* or *Ldlr-/-* mice subjected to a HFD for a maximum of 14-26 weeks[64,74,75,85,87,88]. To systematically compare changes during aging, the effect of *Mif*-deficiency on 18-, 30-, 42- and 48-week-old *Apoe-/-* mice which were set on HFD for 12, 24, 36 and 42 weeks, respectively, was investigated.

### 4.1.1 Body weight analysis

The first comparison was applied to the animals' body weights. Body weights of *Apoe-/-* control mice were higher than those of *Apoe-/- Mif-/-* mice at 24 weeks of HFD but did not differ significantly. While the body weights of *Apoe-/-* mice further increased with aging, those of *Apoe-/- Mif-/-* mice decreased or at least remained constant (**Table 17**).

**Table 17: Body weights of *Apoe-/-* and *Apoe-/- Mif-/-* mice after 12, 24, 36 and 42 weeks of HFD**

| | ***Apoe-/-*** | | | ***Apoe-/- Mif-/-*** | | | |
|---|---|---|---|---|---|---|---|
| HFD (weeks) | Weight (g) | SD[1] | n[2] | Weight (g) | SD[1] | n[2] | *P* value |
| 12 | 27.2 | 2.6 | 7 | 29.5 | 2.4 | 6 | 0.859 |
| 24 | 35.4 | 4.8 | 8 | 34.0 | 3.7 | 6 | 0.961 |
| 36 | 37.8 | 6.3 | 7 | 32.1 | 6.0 | 6 | 0.120 |
| 42 | 38.2 | 5.5 | 9 | 32.6 | 3.3 | 8 | 0.057 |

[1]SD, standard deviation; [2]n, number of mice. These experiments were performed together with C. Krammer.

### 4.1.2 Blood parameter analysis

Plasma lipid analyses revealed significantly decreased triglyceride levels upon systemic *Mif*-deficiency at 42 weeks of HFD. Likewise, cholesterol levels were reduced in *Apoe-/- Mif-/-* mice in comparison to *Apoe-/-* mice at 24 and 42 weeks of HFD, but the differences were statistically insignificant (**Table 18**).

Hematologic parameters such as white blood cells (WBCs) or hemoglobin (HGB) were unchanged upon *Mif*-deficiency and aging (**Table 19**).

**Table 18: Plasma cholesterol and triglyceride levels of *Apoe-/-* and *Apoe-/- Mif-/-* mice after 24 and 42 weeks of HFD**

| | | ***Apoe-/-*** | | | ***Apoe-/- Mif-/-*** | | | |
|---|---|---|---|---|---|---|---|---|
| HFD (weeks) | Parameter | Mean | SD[1] | n[2] | Mean | SD[1] | n[2] | *P* value |
| 24 | Cholesterol (mg/dl) | 899.6 | 423.5 | 7 | 670.1 | 274.9 | 7 | 0.296 |
| 42 | Cholesterol (mg/dl) | 1050.4 | 278.3 | 9 | 806.9 | 186.7 | 8 | 0.197 |
| 24 | Triglyceride (mg/dl) | 132.8 | 68.6 | 7 | 134.4 | 59.5 | 6 | 0.999 |
| 42 | Triglyceride (mg/dl) | 211.4 | 88.2 | 7 | 116.9 | 28.9 | 7 | 0.025 |

[1]SD, standard deviation; [2]n, number of mice. These experiments were performed together with C. Krammer.

**Table 19: Hematologic parameters of *Apoe-/-* and *Apoe-/- Mif-/-* mice after 24 and 42 weeks of HFD**

| | | ***Apoe-/-*** | | | ***Apoe-/- Mif-/-*** | | | |
|---|---|---|---|---|---|---|---|---|
| HFD (weeks) | Parameter | Mean | SD[1] | n[2] | Mean | SD[1] | n[2] | *P* value |
| 24 | WBCs[3] ($10^3$/mm$^3$; $10^9$/l) | 3.700 | 1.113 | 5 | 4.100 | 1.220 | 5 | >0.999 |
| | RBCs[4] ($10^3$/mm$^3$; $10^{12}$/l) | 4.385 | 1.885 | 6 | 5.498 | 0.971 | 6 | >0.999 |
| | HGB[5] (g/dl) | 9.350 | 4.079 | 6 | 10.100 | 4.641 | 6 | >0.999 |
| | HCT[6] (%) | 24.167 | 10.816 | 6 | 29.283 | 5.005 | 6 | >0.999 |
| | MCV[7] (µm$^3$; fl) | 54.667 | 3.386 | 6 | 53.333 | 1.366 | 6 | >0.999 |
| | MCH[8] (pg) | 21.283 | 1.539 | 6 | 20.133 | 2.484 | 6 | >0.999 |
| | MCHC[9] (g/dl) | 38.950 | 2.061 | 6 | 37.650 | 3.908 | 6 | >0.999 |
| | MPV[10] (µm$^3$; fl) | 5.900 | 0.505 | 6 | 6.200 | 0.316 | 4 | >0.999 |
| | RDW[11] (%) | 13.833 | 0.647 | 6 | 14.700 | 2.268 | 6 | >0.999 |
| 42 | WBCs[3] ($10^3$/mm$^3$; $10^9$/l) | 3.814 | 1.410 | 7 | 3.812 | 1.389 | 8 | >0.999 |
| | RBCs[4] ($10^3$/mm$^3$; $10^{12}$/l) | 6.230 | 0.794 | 9 | 5.699 | 1.205 | 8 | >0.999 |
| | HGB[5] (g/dl) | 11.844 | 2.210 | 9 | 12.390 | 2.292 | 11 | >0.999 |
| | HCT[6] (%) | 34.350 | 5.334 | 9 | 27.168 | 8.685 | 11 | 0.6 |
| | MCV[7] (µm$^3$; fl) | 52.555 | 1.446 | 9 | 53.625 | 1.188 | 8 | >0.999 |
| | MCH[8] (pg) | 18.044 | 1.573 | 9 | 20.569 | 1.166 | 8 | >0.999 |
| | MCHC[9] (g/dl) | 34.239 | 3.086 | 9 | 38.138 | 1.502 | 8 | >0.999 |
| | MPV[10] (µm$^3$; fl) | 6.400 | 0.240 | 9 | 5.923 | 1.081 | 11 | >0.999 |
| | RDW[11] (%) | 14.172 | 0.602 | 9 | 14.068 | 0.792 | 8 | >0.999 |

[1]SD, standard deviation; [2]n, number of mice; [3]WBCs, white blood cells; [4]RBCs, red blood cells; [5]HGB, hemoglobin; [6]HCT, hematocrit; [7]MCV, mean corpuscular volume; [8]MCH, mean corpuscular hemoglobin; [9]MCHC, mean corpuscular hemoglobin concentration; [10]MPV, mean platelet volume; [11]RDW, red blood cell distribution width. These experiments were performed together with C. Krammer.

### 4.1.3 Analysis of atherosclerotic lesion size

Atherosclerotic lesion size was analyzed at different sites of the aorta and branching arteries and the previously described site-specific atheroprotective phenotype due to *Mif*-deficiency could be reconstructed[85]. *Apoe-/- Mif-/-* mice displayed a significantly diminished lesion size compared to *Apoe-/-* mice after 24 weeks of HFD in the innominate artery and AA (**Figure 14A,B,E,H**), but not in the other aortic vascular regions (**Figure 14C-G**). Surprisingly, atheroprotection was lost throughout the process of aging and exposure to HFD. The effect of *Mif* gene deletion on plaque size was still apparent in the BCA and the AA after 36, but not 42 weeks of HFD (**Figure 14A,B,E,H**).

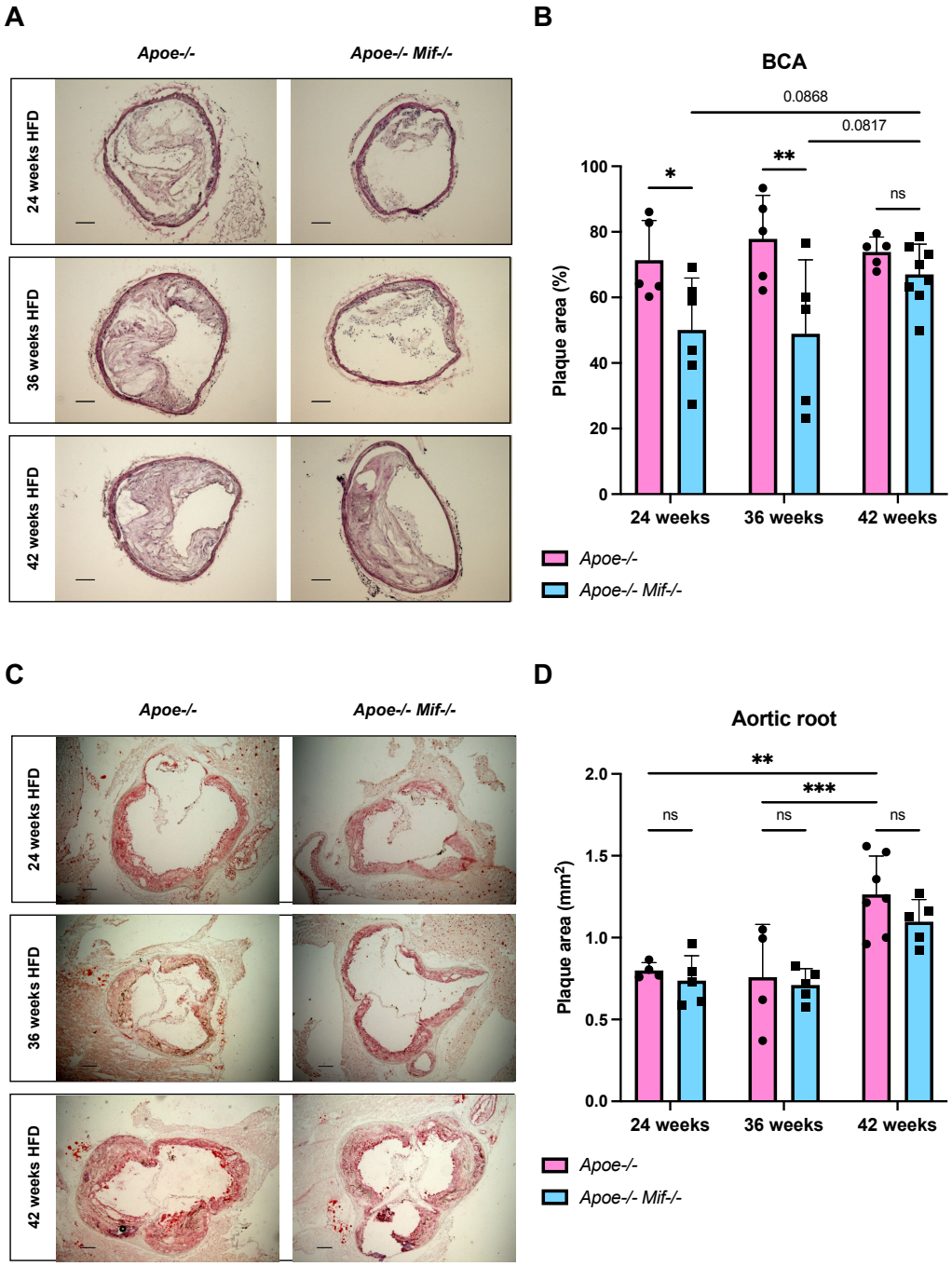


**Figure 14a: Vascular region-specific atheroprotection owing to *Mif*-deficiency is lost in aged *Apoe-/-* mice**. Atherosclerotic plaques were quantified in innominate artery and aortic root of *Apoe-/-* mice (pink) compared to *Apoe-/- Mif-/-* mice (blue), respectively after the indicated HFD intervals. **A-B)** Representative images **(A)** and plaque quantification **(B)** of H&E-stained BCA sections. For each mouse, mean values of 12 serial sections, spaced 50 µm apart, were calculated. The plaque area is depicted as percentage of the overall inner vessel area (n=5-8, results are shown as means ± SD; scale: 100 µm). **C-D)** Representative images **(C)** and plaque quantification **(D)** of ORO-stained sections of the aortic root. Serial sections were generated as in **(A-B)**. The plaque area is depicted in $mm^2$ (n=4-7, results are shown as means ± SD; scale: 200 µm). Statistics: two-way ANOVA; *, $P<0.05$; **, $P<0.01$; ***, $P<0.001$; ns, non-significant; non-significant results with $P$ values between 0.05 and 0.1 are presented as precise numbers; each data point is one mouse. These experiments were performed together with C. Krammer.

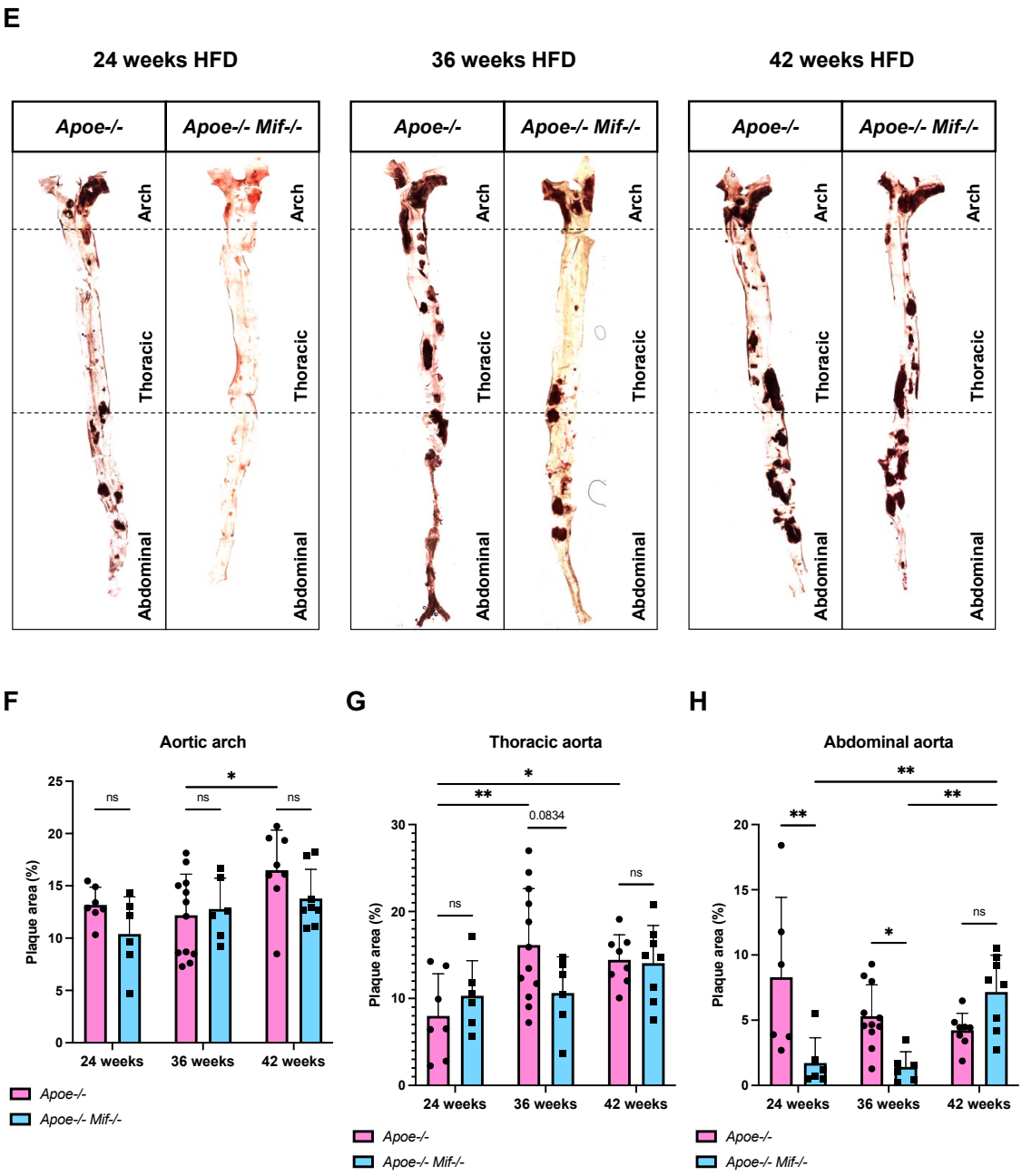


**Figure 14b: Vascular region-specific atheroprotection owing to *Mif*-deficiency is lost in aged *Apoe-/-* mice.** Atherosclerotic plaques were quantified in aortic arch, thoracic aorta and abdominal aorta of *Apoe-/-* mice (pink) compared to *Apoe-/- Mif-/-* mice (blue), respectively after the indicated HFD intervals. **E-H)** Representative images of *en face*-prepared and ORO-stained aortas **(E)** and plaque quantification in aortic arch **(F)**, thoracic aorta **(G)** and abdominal aorta **(H)**. The plaque area is depicted as percentage of the overall aortic surface (n=6-12, results are shown as means ± SD). Statistics: for details see Figure 14a. These experiments were performed together with C. Krammer.

### 4.1.4 Preliminary study indicates no effect of *Mif*-deficiency in the 12 weeks HFD-setting

Atherosclerotic lesion size was also analyzed in the 12 weeks HFD-setting, comparing *Apoe-/-* with *Apoe-/- Mif-/-* mice. Here, no significant differences were observed between groups, neither in BCA nor in arch, thoracic aorta or AA (**Figure 14J-K**). Due to a limited number of mice, these results are preliminary.

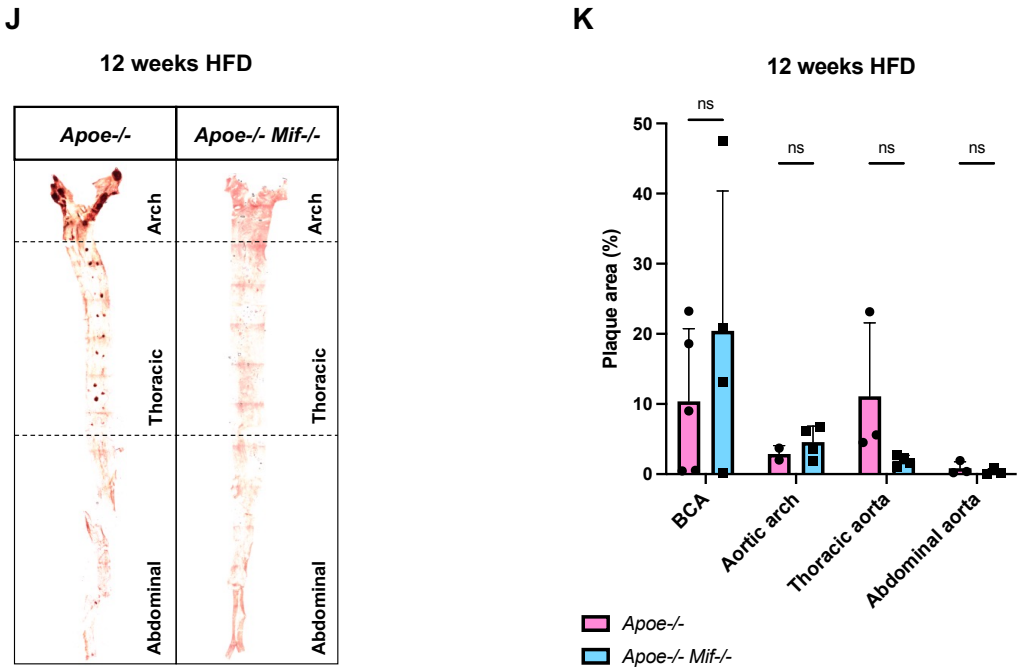


**Figure 14c: Preliminary study indicates no effect of *Mif*-deficiency in the 12 weeks HFD-setting.** Atherosclerotic plaques were quantified in BCA, aortic arch, thoracic aorta and abdominal aorta of *Apoe-/-* mice (pink) compared to *Apoe-/- Mif-/-* mice (blue) after 12 weeks of HFD. **J-K)** Representative images of *en face*-prepared and ORO-stained aortas **(J)** and plaque quantification **(K)**. The plaque area is depicted as percentage of the overall aortic surface (n=2-5, results are shown as means ± SD). Statistics: for details see Figure 14a.

Combined, the data show that, in the *Apoe-/-* background, *Mif*-deficiency reduces atherosclerotic lesion size after 24 and 36 weeks of HFD, but not yet after 12 weeks and no longer after 42 weeks of HFD. Simultaneously, serum triglyceride levels and body weights were reduced in 42 weeks HFD-fed *Apoe-/- Mif-/-* mice. Further blood parameters were unaltered between groups.

## 4.2 *Mif*-deficiency affects peripheral and splenic immune cell profiles during aging

*In the following section, Figure 15a and 15b have already been published in part in the peer reviewed FASEB J publication by Krammer, Yang, Reichl et al. 2023 and the corresponding preprints.*

The identified MIF- and age-dependent lesion phenotype gives rise to the question about the underlying mechanisms. To start with, the overall immune profile was investigated in blood, spleen, BM and LNs. Leucocyte subsets, including T cells, B cells, neutrophils, and monocytes, were compared in *Apoe-/-* and *Apoe-/- Mif-/-* mice after 12, 24, 36 and 42 weeks of HFD.

### 4.2.1 *Mif*-deficiency increases splenic CD4+ T cell numbers during aging

Flow cytometric analyses revealed decreased T cell numbers in blood, BM and LNs of *Apoe-/- Mif-/-* mice compared to *Apoe-/-* mice at 12 and 24 weeks of HFD (**Figure 15A,C,D**). Concurrently, a trend towards decreased peripheral CD4+ T cell numbers could be observed (**Figure 15A**).

Splenic T cell amounts were increased in *Apoe-/- Mif-/-* mice compared to *Apoe-/-* mice at 12 and 24 weeks of HFD and to the greatest extent at 42 weeks of HFD. In particular, CD4+ T cells were affected (**Figure 15B**).

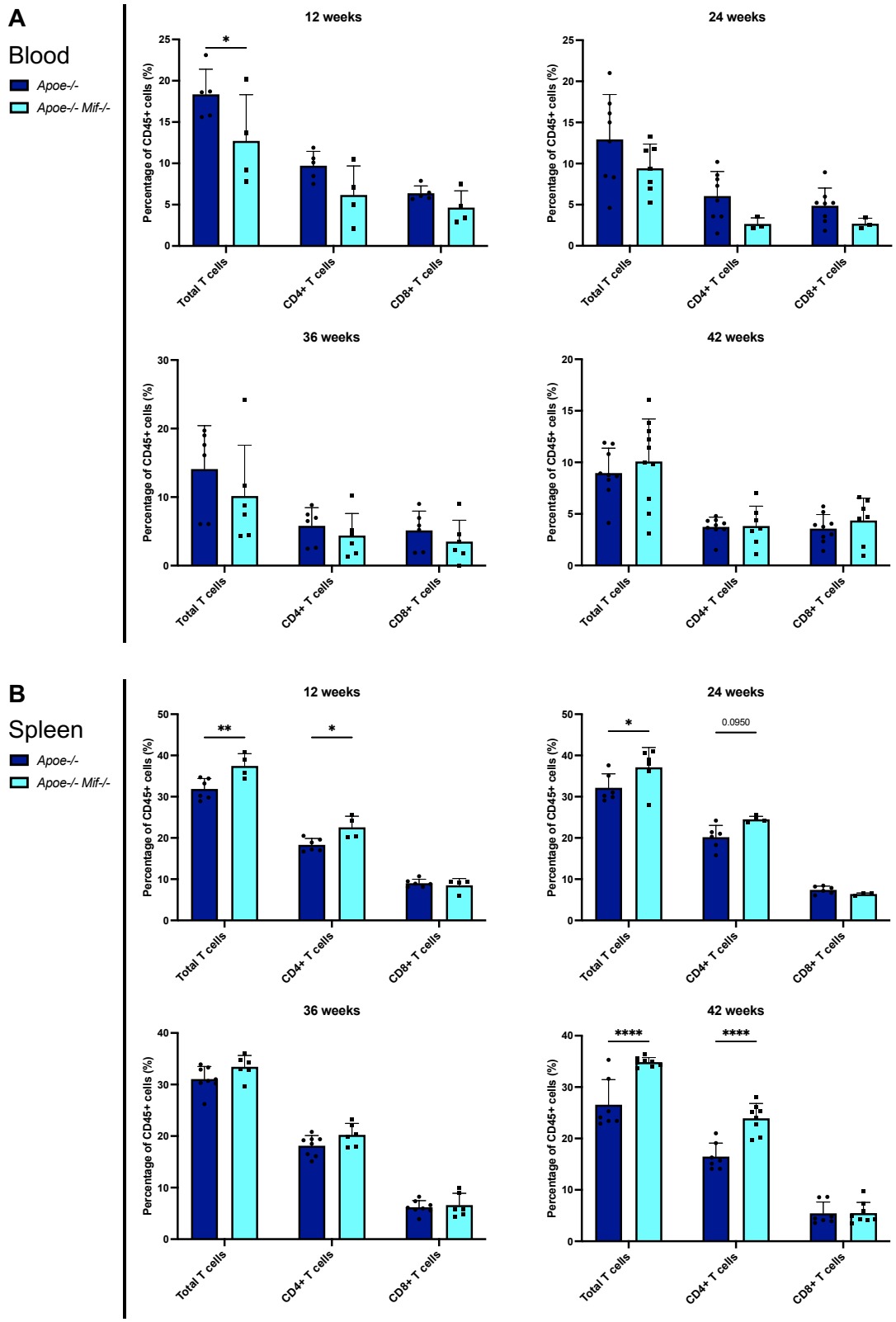


**Figure 15a: *Mif*-deficiency increases splenic CD4+ T cell numbers during aging.** FACS-based quantification of total T cells, CD4+ T cells and CD8+ T cells in blood **(A)** and spleen **(B)** of *Apoe-/- Mif-/-* mice (light blue) compared to *Apoe-/-* control mice (dark blue). Mice were respectively examined after 12, 24, 36 and 42 weeks of HFD. Results are shown as means ± SD, each data point is one mouse (n=6-11). Statistics: two-way ANOVA; *, $P<0.05$; **, $P<0.01$; ****, $P<0.0001$; non-significant results with $P$ values between 0.05 and 0.1 are presented as precise numbers. These experiments were performed with assistance from C. Krammer.

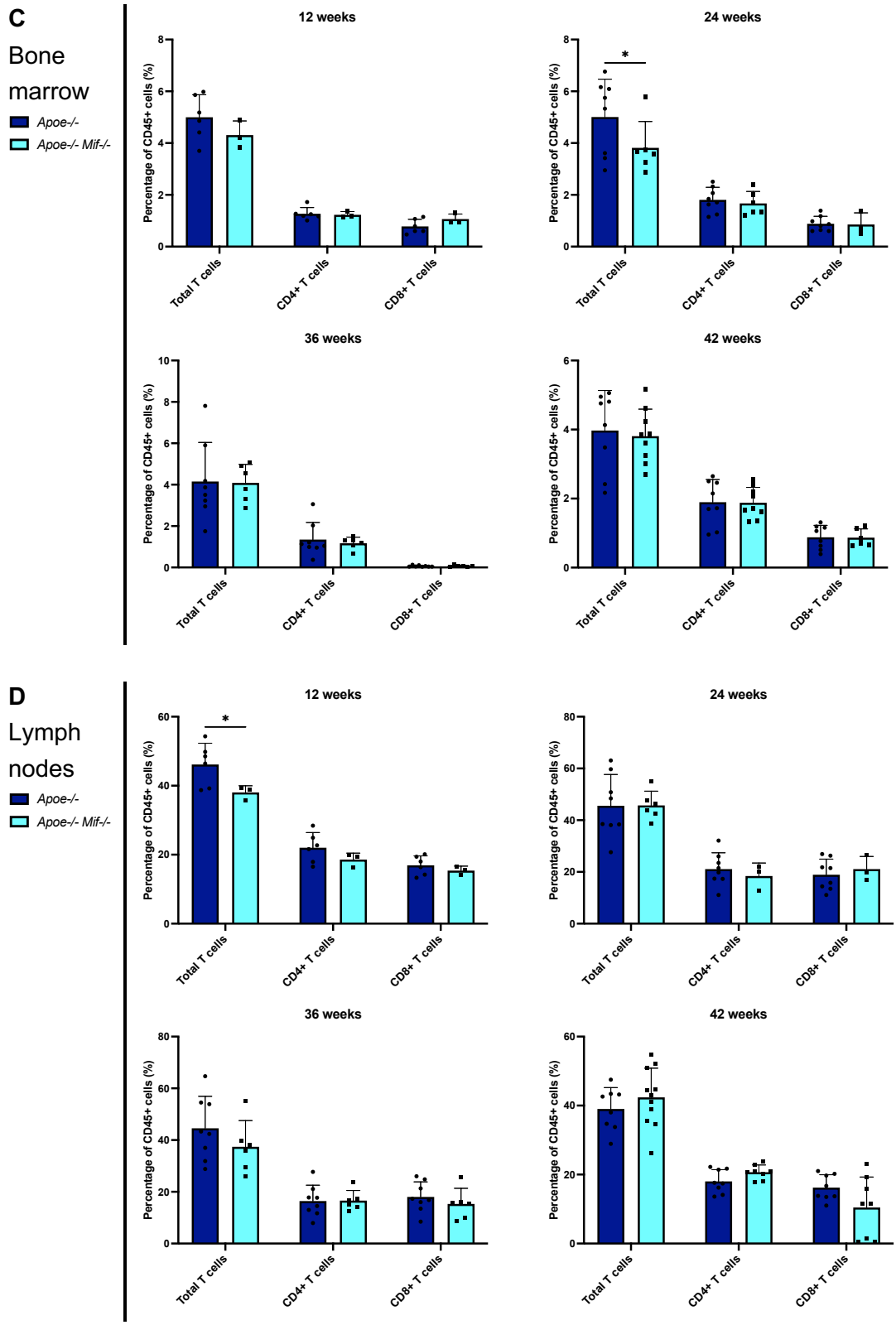


**Figure 15b: *Mif*-deficiency increases splenic CD4+ T cell numbers during aging.** FACS-based quantification of total T cells, CD4+ T cells and CD8+ T cells in bone marrow **(C)** and lymp nodes **(D)** of *Apoe-/- Mif-/-* mice (light blue) compared to *Apoe-/-* control mice (dark blue). Mice were respectively examined after 12, 24, 36 and 42 weeks of HFD. Results are shown as means ± SD, each data point is one mouse (n=6-11). Statistics: for details see Figure 15a. These experiments were performed with assistance from C. Krammer.

### 4.2.2 *Mif*-deficiency increases B2 and decreases B1 B cell numbers in blood during aging

Total B cell numbers were not affected, neither in a MIF- nor in an age-dependent manner (**Figure 16A-D**).

B2 B cell amounts were significantly increased in blood of *Apoe-/- Mif-/-* mice compared to *Apoe-/-* mice at all time points with the most distinctive difference at 42 weeks of HFD (**Figure 16A**). In spleen and LNs, B2 B cell numbers were reduced upon *Mif*-deficiency after 24 weeks of HFD, but slightly or significantly elevated after 42 weeks of HFD (**Figure 16B,D**).

Peripheral B1 B cells, respectively B1b B cells, were slightly diminished in 12, 24 and 36 weeks HFD-fed *Apoe-/- Mif-/-* mice compared to *Apoe-/-* controls reaching statistical significance after 42 weeks of HFD (**Figure 16A**).

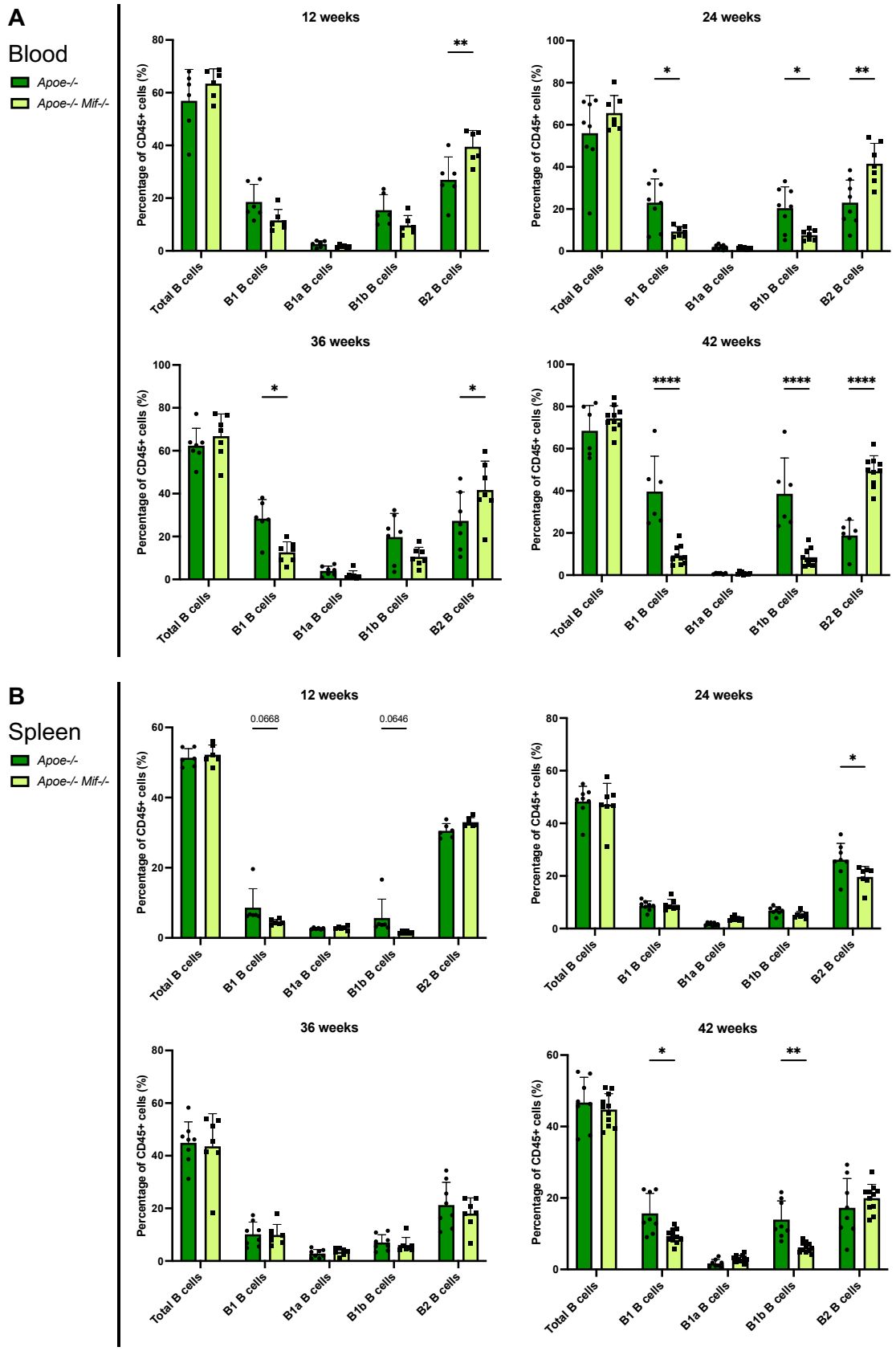


**Figure 16a: *Mif*-deficiency increases B2 and decreases B1 B cell numbers in blood during aging.** FACS-based quantification of total B cells, B1 B cells, B1a B cells, B1b B cells and B2 B cells in blood **(A)** and spleen **(B)** of *Apoe-/- Mif-/-* mice (light green) compared to *Apoe-/-* control mice (dark green). Mice were respectively examined after 12, 24, 36 and 42 weeks of HFD. Results are shown as means ± SD, each data point is one mouse (n=6-11). Statistics: two-way ANOVA; *, $P<0.05$; **, $P<0.01$; ****, $P<0.0001$; non-significant results with $P$ values between 0.05 and 0.1 are presented as precise numbers.

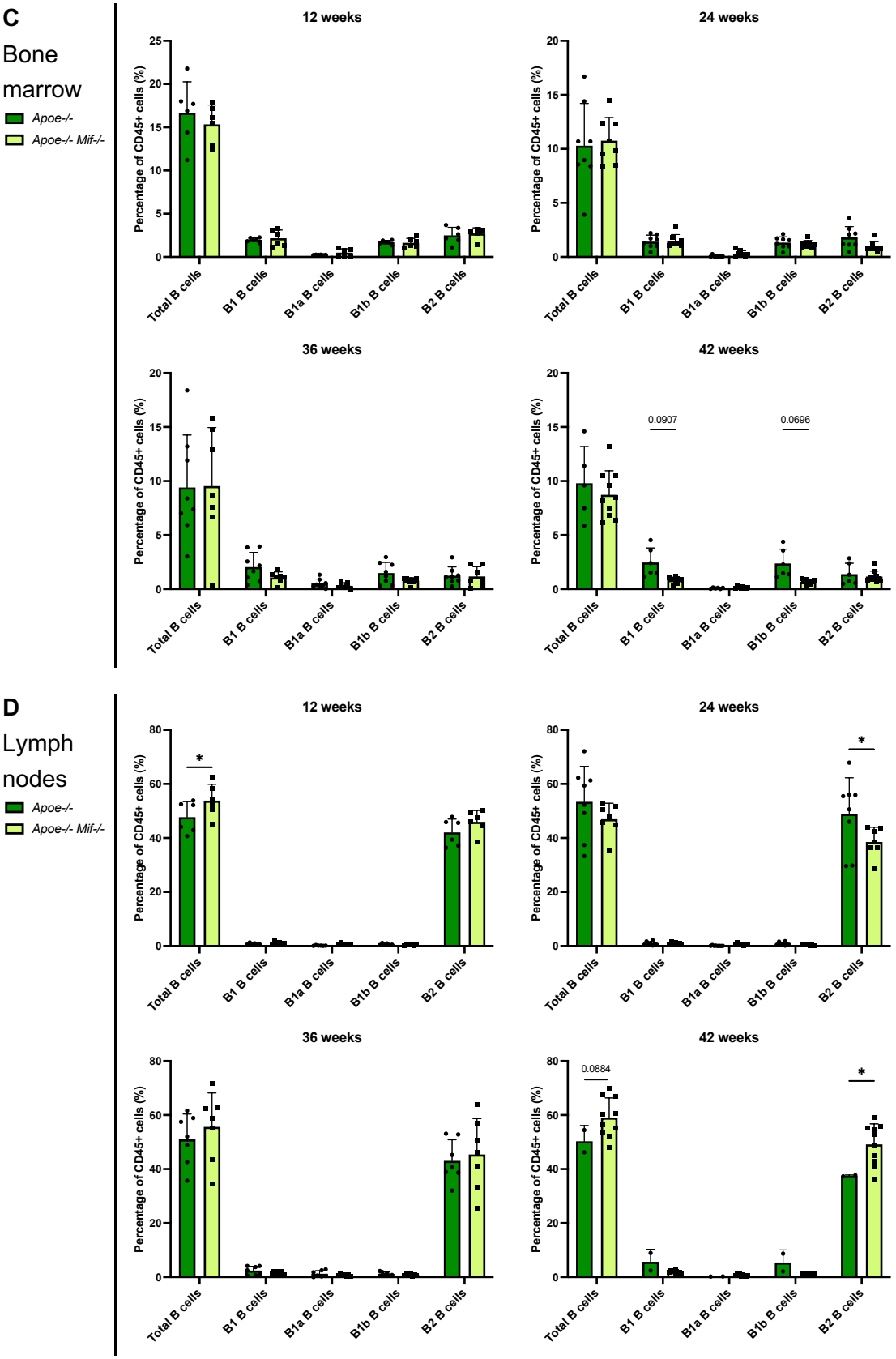


**Figure 16b: *Mif*-deficiency increases B2 and decreases B1 B cell numbers in blood during aging.** FACS-based quantification of total B cells, B1 B cells, B1a B cells, B1b B cells and B2 B cells in bone marrow **(C)** and lymph nodes **(D)** of *Apoe-/- Mif-/-* mice (light green) compared to *Apoe-/-* control mice (dark green). Mice were respectively examined after 12, 24, 36 and 42 weeks of HFD. Results are shown as means ± SD, each data point is one mouse (n=2-10). Statistics: for details see Figure 16a.

### 4.2.3 *Mif*-deficiency does not change myeloid cell numbers in blood or spleen during aging

Regarding myeloid cell numbers, no MIF- or age-dependent alterations were seen in blood or spleen (**Figure 17A-B**).

Neutrophil counts were elevated in BM of 12 and 24 weeks HFD-fed *Apoe-/- Mif-/-* mice compared to *Apoe-/-* mice, but the changes were not mirrored in blood, spleen or LNs (**Figure 17A-D**). Besides, the impact of *Mif*-deficiency on neutrophil amounts was restricted to LNs at 36 weeks of HFD (**Figure 17D**).

Monocyte numbers were increased in LNs of *Apoe-/- Mif-/-* mice compared to *Apoe-/-* mice after 12 and 24 weeks of HFD (**Figure 17D**). As these changes did not give rise to mechanisms causing the observed phenotype, they were not further pursued.

Summing up, the data support the notion that *Mif*-deficiency affects splenic T-cell and peripheral B-cell subgroup numbers upon aging. Myeloid cell numbers were influenced only at selective time points in bone marrow and lymph nodes, and not at all in blood or spleen.

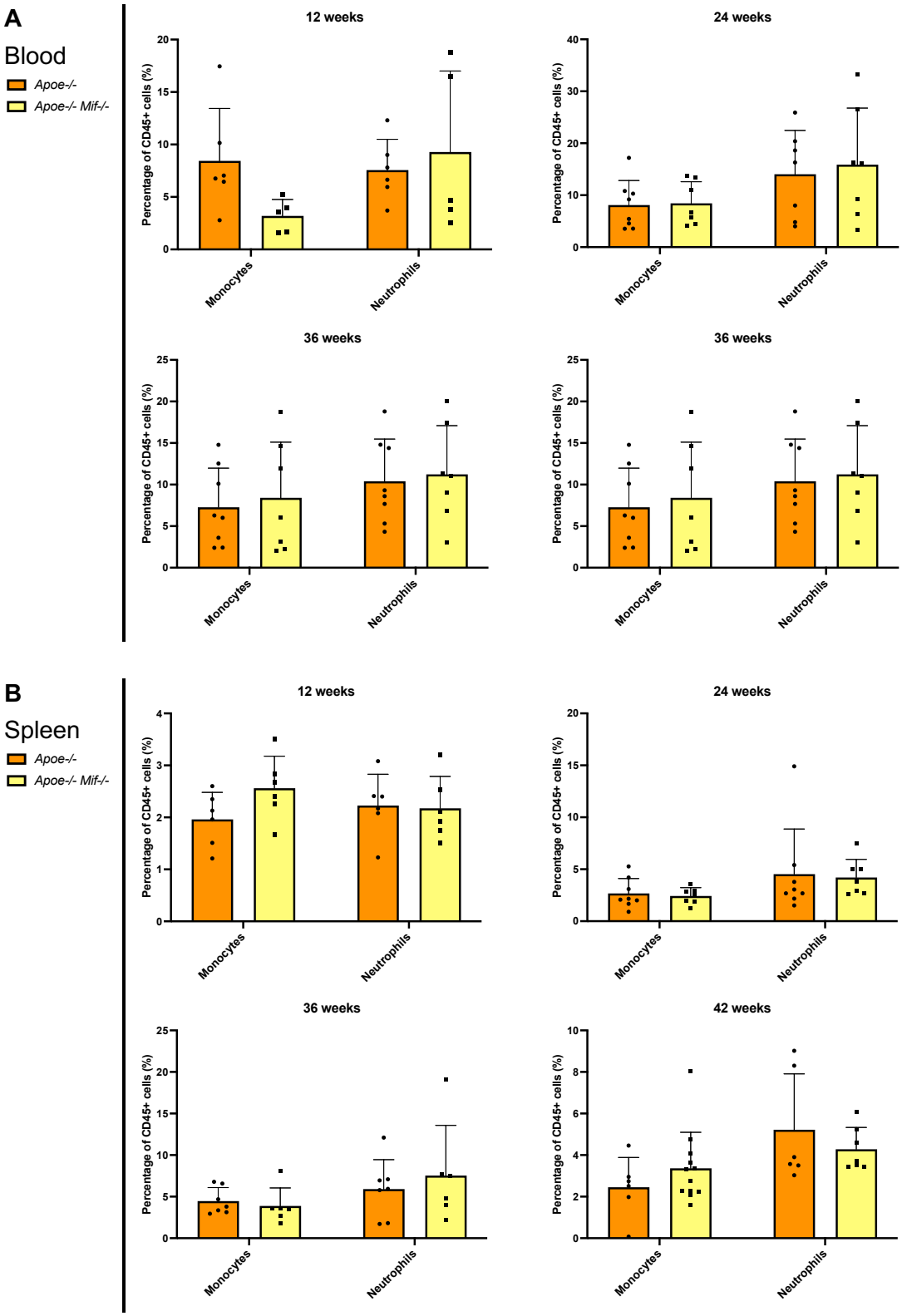


**Figure 17a: *Mif*-deficiency does not change myeloid cell numbers in blood or spleen during aging**. FACS-based quantification of monocytes and neutrophils in blood **(A)** and spleen **(B)** of *Apoe-/- Mif-/-* mice (yellow) compared to *Apoe-/-* control mice (orange). Mice were respectively examined after 12, 24, 36 and 42 weeks of HFD. Results are shown as means ± SD, each data point is one mouse (n=5-12). Statistics: two-way ANOVA; *, $P<0.05$; **, $P<0.01$; ****, $P<0.0001$; non-significant results with $P$ values between 0.05 and 0.1 are presented as precise numbers.

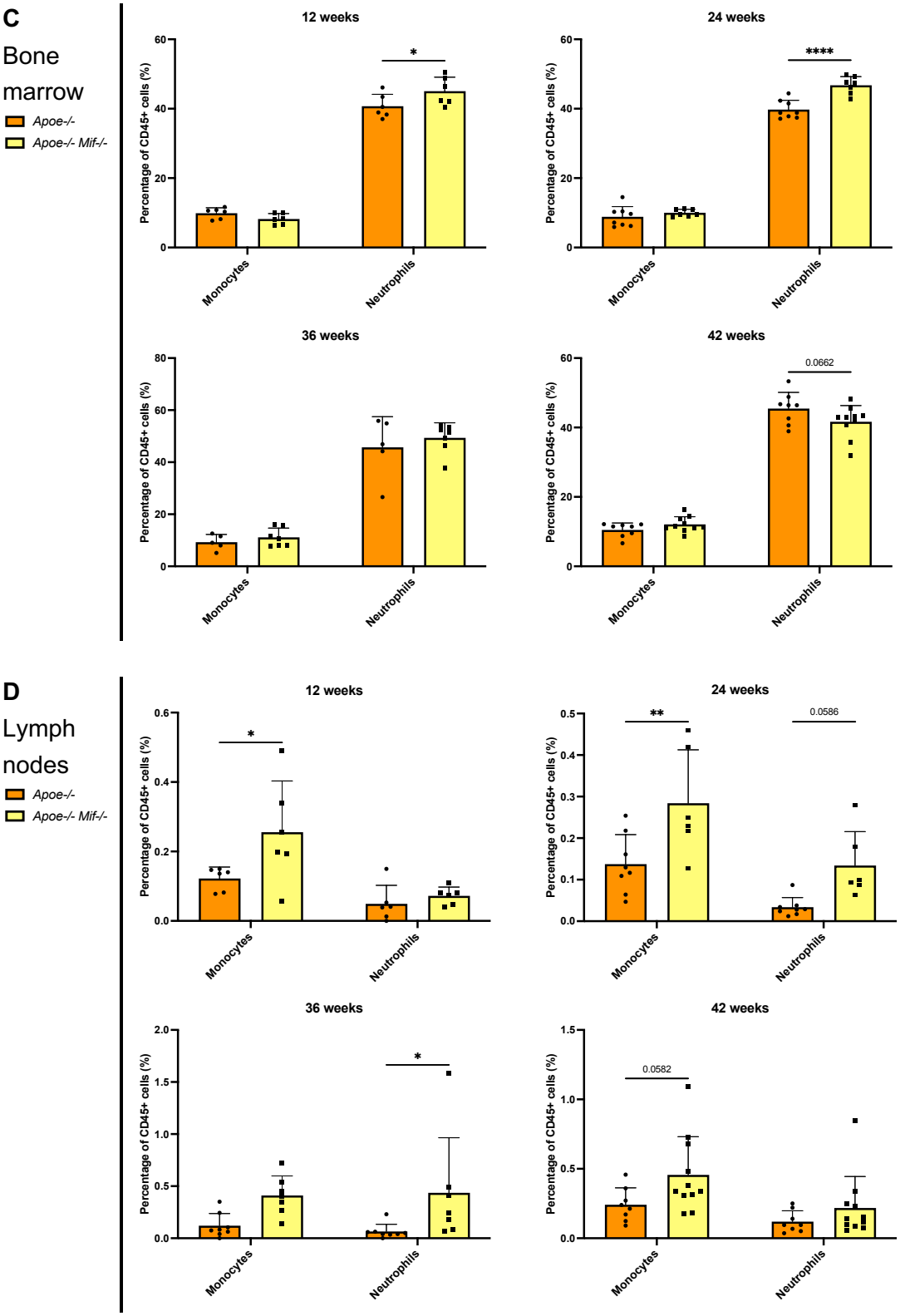


**Figure 17b: *Mif*-deficiency does not change myeloid cell numbers in blood or spleen during aging.** FACS-based quantification of monocytes and neutrophils in bone marrow **(C)** and lymph nodes **(D)** of *Apoe-/- Mif-/-* mice (yellow) compared to *Apoe-/-* control mice (orange). Mice were respectively examined after 12, 24, 36 and 42 weeks of HFD. Results are shown as means ± SD, each data point is one mouse (n=5-11). Statistics: for details see Figure 17a.

## 4.3 *Mif*-deficiency favors re-distribution of B cells in atheroprotective stage I ATLOs in *Apoe-/-* mice, but not at an advanced age

*In the following section, Figure 18 has already been published in part in the peer reviewed FASEB J publication by Krammer, Yang, Reichl et al. 2023 and the corresponding preprints.*

### 4.3.1 *Mif*-deficiency accelerates B cell cluster formation

Recently, B cells have been shown to accumulate in peri-adventitial clusters, adjacent to atherosclerotic lesions, upon *Mif*-deficiency in relatively younger mice[85]. Considering the loss of vascular region-specific atheroprotection owing to *Mif*-deficiency in aged *Apoe-/-* mice, I hypothesized that B cell clustering is also altered over the course of aging.

Immunostaining against B220 revealed the presence of peri-adventitial B cell clusters in the BCA of *Apoe-/- Mif-/-* mice, but not *Apoe-/-* control mice, after 24 weeks of HFD (**Figure 18A-B**). In fact, the number of detected clusters increased in *Apoe-/-* mice until 42 weeks of HFD, while cluster formation stagnated in *Apoe-/- Mif-/-* mice (**Figure 18B**).

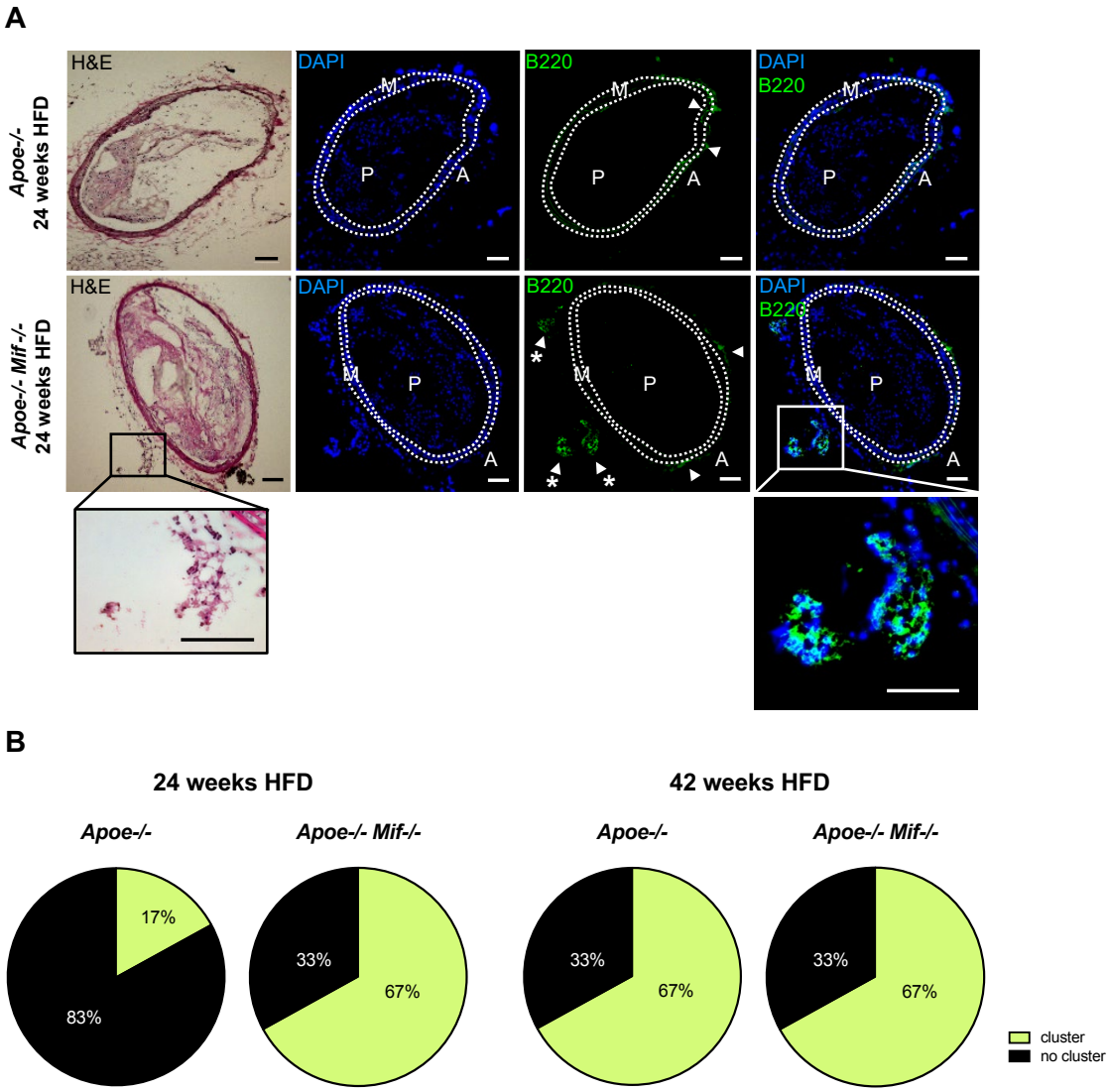


**Figure 18: *Mif*-deficiency accelerates B cell cluster formation.** B cell-rich peri-adventitial cell clusters were identified in the BCA of *Apoe-/-* mice compared to *Apoe-/- Mif-/-* mice, respectively after 24 and 42 weeks of HFD (n=6 mice per group). For each mouse, 10 serial sections, spaced 50 µm apart, were analyzed. **A)** Representative images of H&E staining and immunostaining against B220 on BCA sections after 24 weeks of HFD. Nuclei were counterstained with DAPI. Arrows indicate B cells, arrows combined with an asterisk indicate B cell clusters. A=adventitia, M=media, P=Plaque; scale: 100 µm. **B)** Quantification of the detected B cell clusters.

### 4.3.2 The identified clusters in *Apoe-/- Mif-/-* mice show characteristics reminiscent of early-stage ATLOs

Adventitial assemblages of immune cells have been described in the context of ATLOs emerging in aged atherogenic *Apoe-/-* mice[37]. As the identified clusters in the innominate artery of *Apoe-/- Mif-/-* mice could represent early ATLOs, I characterized their cellular composition.

ATLOs can be identified through markers of classifying structures. Here, immunostainings against B220, CD3e, Lyve-1, CXCL13 and Collagen type IV revealed the presence of B cells, T cells, lymph vessels, CXCL13 as a B cell recruitment factor and connective tissue. Besides, the clusters displayed sparse ER-TR7 positivity.

However, structures indicative of fully developed ATLOs were missing, as peripheral node addressin (PNAd) and CD35 as markers of HEVs and FDCs, could not be addressed by staining, implying earlier stages of ATLOs (**Figure 19**).

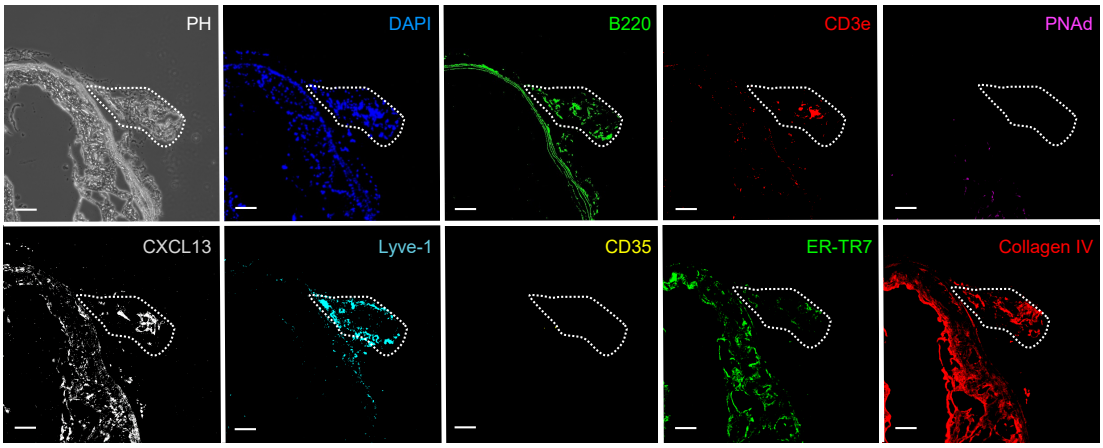


**Figure 19: The identified clusters in *Apoe-/- Mif-/-* mice show characteristics reminiscent of early-stage ATLOs.** Representative images of immunostaining against ATLO-classifying markers comprising B220 (B cells), CD3e (T cells), PNAd (HEVs), CXCL13, Lyve-1 (lymph vessels), CD35 (FDCs), ER-TR7 (reticular fibroblasts and fibres) and CollagenIV on clusters of *Apoe-/- Mif-/-* mice at 24 weeks of HFD. The phase-contrast (PH) image is shown for better orientation. Nuclei were counterstained with DAPI. The circled regions indicate the analyzed cluster. Scale: 50 µm.

Altogether, the data point to an accelerated B cell cluster formation in the adventitia of *Mif*-deficient compared to *Mif*-proficient *Apoe-/-* mice. These B cell-rich clusters were shown to harbor hallmarks of early ATLOs.

## 4.4 Plasma anti-oxLDL IgM antibody titers are lower in older *Apoe-/- Mif-/-* mice

*In the following section, Figure 20 has already been published in part in the peer reviewed FASEB J publication by Krammer, Yang, Reichl et al. 2023 and the corresponding preprints.*

The prevailing early ATLOs in 24 weeks HFD-fed *Apoe-/- Mif-/-* mice could protect from atherogenesis as B cells originating from ATLOs have been assumed to do so[39]. B cells, especially B1 B cells, mediate their atheroprotective functions by producing natural IgM antibodies[26]. In contrast, B2 B cells produce mainly pathogenic IgG antibodies[27]. Thus, I examined the circulating levels of oxLDL-directed IgM versus IgG antibodies.

Anti-oxLDL IgM levels were significantly lower in *Apoe-/- Mif-/-* mice in comparison to *Apoe-/-* mice after 42 weeks of diet (**Figure 20A**), whereas anti-oxLDL IgG isotype levels did not differ significantly (**Figure 20B**). At 24 weeks of HFD, anti-oxLDL IgM antibody titers were stable upon *Mif*-deficiency (**Figure 20A**).

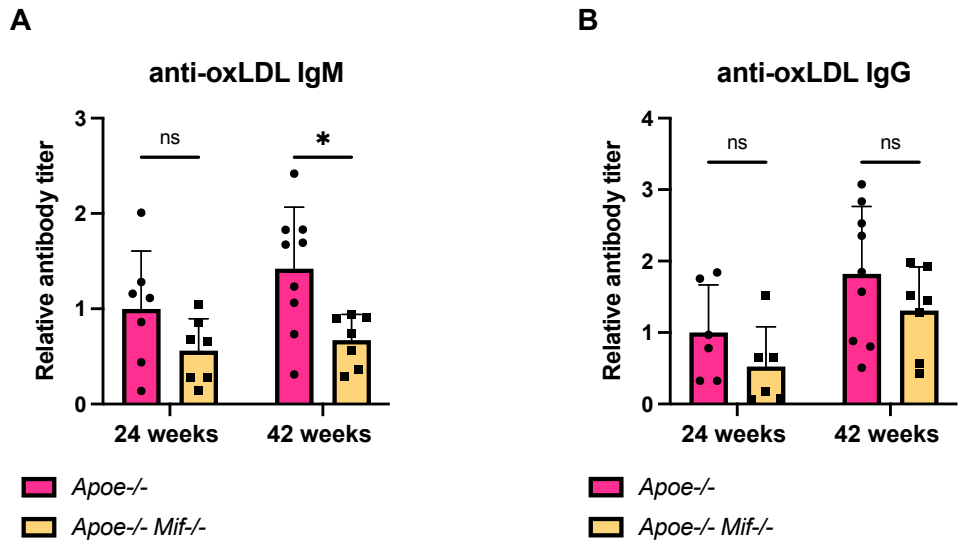


**Figure 20: Plasma anti-oxLDL IgM antibody titers are lower in older *Apoe-/- Mif-/-* mice.** Circulating levels of anti-oxLDL IgM **(A)** and IgG **(B)** in *Apoe-/-* mice (pink) compared to *Apoe-/- Mif-/-* mice (orange), respectively after 24 and 42 weeks of HFD. A modified ELISA was performed and measured values were normalized to those of the 24 weeks HFD-fed *Apoe-/-* mouse group. Results are shown as means ± SD, each data point is one mouse (n=6-9). Statistics: two-way ANOVA; *, $P<0.05$; ns, non-significant.

# 5. Discussion

Macrophage migration inhibitory factor (MIF) is a non-canonical inflammatory mediator that promotes atherogenesis through its interaction with the classical chemokine receptors CXCR2 and CXCR4 mediating the recruitment of monocytes and T cells, respectively[50,64]. This MD thesis contributed numerous lines of evidence to establish a connection between MIF and age-related effects in atherogenesis, displaying the loss of vascular site-specific atheroprotection in *Mif*-deficient pro-atherogenic *Apoe-/-* mice throughout the process of aging and exposure to HFD. As underlying mechanisms, I found a relatively decreasing frequency of B cell-rich early-stage ATLO-like clusters and reduced levels of plasma anti-oxLDL IgM antibodies in aged *Apoe-/- Mif-/-* mice compared to *Apoe-/-* control mice. **Figure 21** gives an overview of these mechanisms and their impacts on atheroprotection.

MIF exerts pro-inflammatory and atherogenic properties as demonstrated in experimental studies utilizing *Mif* gene deletion in *Ldlr-/-* mice or antibody blockade in *Apoe-/-* mice on a Western-type HFD[64,74,75,85,87,88]. In line, MIF levels correlate with human atherosclerotic disease and CAD[72,73].

The link between MIF and the pathogenesis of atherosclerotic lesions in relation to the aging process has not been studied so far. Indeed, a maximum of 14-26 weeks of HFD has been applied to atherogenic mouse models[64,74,75,85,87,88].

Therefore, the consequence of global *Mif*-deficiency on pro-atherogenic *Apoe-/-* mice throughout various stages of aging and HFD was analyzed. Wildtype *Apoe-/-* mice were compared to *Apoe-/- Mif-/-* mice after 18, 30, 42 and 48 weeks of age, i.e. 12, 24, 36 and 42 weeks of HFD, respectively.

*Mif* gene deletion in the hyperlipidemic *Ldlr-/-* model results in reduced plaque sizes across the total vasculature comprising innominate artery, aortic root, aortic arch, thoracic aorta and AA[74]. In contrast, *Mif* gene deletion in an *Apoe-/-* background features vascular site-specific atheroprotection with lesion reduction limited to the BCA and AA[85]. The underlying mechanisms have not been determined so far.

Here, I confirmed the regio-specific atheroprotective phenotype in 30-week-old *Apoe-/- Mif-/-* mice on HFD for 24 weeks, which was found to be lost after 42 weeks of HFD. In line, a recently established model of 52-week-old mice, with restriction of HFD to the final 6 weeks, did not display an atheroprotective phenotype upon *Mif*-deficiency[89]. In the 12 weeks HFD-setting, preliminary results indicate no effect of *Mif* gene deletion. Simultaneously, *Apoe-/- Mif-/-* mice on HFD for 42 weeks exhibited significantly lower serum lipid levels and a tendency towards decreased body weights compared to *Apoe-/-* control mice. Thus, metabolic mechanisms as a main cause for the loss of atheroprotection over the course of aging can be excluded. Apparently, atheroprotective mechanisms that are suppressed in *Mif*-proficient mice reappear in *Mif*-deficient mice. In highly aged mice, generally increased inflammation seems to outweigh atheroprotective mechanisms, even upon *Mif*-deficiency. Indeed, inflammatory cytokines like IL-6 or IL-

1ß, which have been attributed atherosclerosis-boosting properties, have been found to grow in number during aging[90,91].

Further analysis of immune cell populations in the circulation and in SLOs suggested that B and T cell numbers may be regulated in a MIF- and age-dependent manner. Lower T cell numbers in blood, BM and LNs as well as a trend towards decreased peripheral CD4+ T cell counts in *Apoe-/- Mif-/-* mice compared to *Apoe-/-* mice after 12 and 24 weeks of HFD match the observed atheroprotective phenotype in 24 weeks HFD-fed *Apoe-/- Mif-/-* mice. Among T cell populations, CD4+ T cells are the key players in inflammation and atherogenesis[9]. Previous studies have shown that CD4+T cell amount and functions are limited in the spleen of aged mice[92,93]. Here, instead, splenic CD4+ T cell counts were increased in *Apoe-/- Mif-/-* mice compared to *Apoe-/-* controls at 12 and 24 weeks of HFD and to the greatest extent at 42 weeks of HFD indicating that *Mif*-deficiency favors T cell homing to the spleen. However, these findings cannot sufficiently explain the witnessed atherosclerotic phenotype in *Mif*-deficient mice and its alteration with aging.

Regarding B cells, developmental studies point to a disrupted shift from immature to transitional B cells upon *Mif*-deficiency, leading to decreased splenic and peripheral B cell counts in *Apoe-/- Mif-/* mice compared to *Apoe-/-* mice[85]. However, B cell numbers itself seem not to account for the atheroprotective effect, as B cell amounts in the vessels were not diminished[85]. In my study, I could not confirm the MIF-dependent decline in total B cells, neither in blood, nor in spleen, BM or LNs. The decisive point might be the presence of different B cell subpopulations.

B cells have been attributed both atherosclerosis-cushioning and -exacerbating functions, uncovered by reconstitution of splenectomized *Apoe-/-* and irradiated *Ldlr-/-* mice with B cell-deficient BM[14,15], and by B cell depletion in *Apoe-/-* and *Ldlr-/-* mice[13,16].

B2 B cells are considered to promote atheroprogression by producing various antibodies[27]. They can be equated with FO B cells as they make up the majority of circulating B2 B cells[17]. As expected, B2 B cell numbers were diminished in spleen and LNs of the double-knockout mice compared to *Apoe-/-* controls after 24 weeks, but elevated after 42 weeks of HFD, indicating a decreased B2 B cell activity upon *Mif*-deficiency which increases with age. Interestingly, B2 B cell counts were heightened in blood of *Apoe-/- Mif-/-* mice compared to *Apoe-/-* mice at all time points, implying the involvement of other B2 B cell function drowning effects in relatively younger *Mif*-deficient mice. During the process of aging, peripheral B2 B cell levels have risen in *Mif*-deficient compared to *Mif*-proficent mice reaching the most distinctive difference at 42 weeks of HFD. Given the lack of atheroprotection in 42 weeks diet-fed *Apoe-/- Mif-/-* mice, B2 B cell levels seem to outweigh atheroprotective effects here.

Regarding anti-atherogenic B cell subgroups, B1 B cells are considered to produce natural IgM antibodies that neutralize oxLDL in atherogenesis[26,27]. Here, B1 B cell amounts were decreased in blood of *Mif*-deficient compared to *Mif*-proficient mice at all time points, but with the main difference at 42 weeks of HFD.

In conclusion, the atheroprotective effect in *Mif*-deficient mice following 24 weeks of HFD was observed in spite of higher B2 B cell and lower B1 B cell levels in the periphery compared to *Apoe-/-* controls. At 42 weeks of HFD, the major discrepancy between B2 B cell and B1 B cell levels has probably exceeded unknown protective mechanisms. Hence, B cell subtypes in blood and SLOs might only play a minor role, which draws focus on B cell behavior in the diseased wall.

Recently, B cells have been shown to accumulate in peri-adventitial clusters near atherosclerotic lesions in the BCA of *Mif*-deficient *Apoe-/-* mice[85]. In my study, I provide evidence that *Mif* deletion accelerates B cell cluster formation in *Apoe-/-* mice only until a certain age. The effect vanishes with aging, in parallel with site-specific atheroprotection.

A detailed description of the cluster composition had not been given. Here, I show that B cell clusters in the BCA of 24 or 42 weeks HFD-fed *Apoe-/- Mif-/-* mice correspond to incipient ATLOs, equivalent to an early-stage cluster. In line with previous studies[36], I found ATLOs also in the BCA of 42 weeks HFD-fed *Apoe-/-* mice.

ATLOs are lymphoid aggregates in the adventitia of aged hyperlipidemic mice close to inflammation sites, which vary from loose T and B cell aggregates to structured lymphoid tissues with distinct immune cell compartments. According to the expression of diverse markers, three consecutive stages can be classified[37,38]. Stage I is distinguished by relatively sparse T and B cell infiltration via the vasa vasorum, while stage II ATLOs are composed of discrete T and B cell areas and the presence of lymph vessels and HEVs[38]. Stage III is hallmarked by large T cell follicles, DCs, B cell follicles with ectopic GCs and proliferating B cells as well as plasma cell niches in the periphery[37,38]. As I detected B cells, T cells and Lyve-1+ lymph vessels within the clusters, while mature features like HEVs and GCs with FDCs were absent, I suspect a stage I or II ATLO with the potential to progress into a stage III ATLO as aging continues. The sparse ER-TR7 positivity of the clusters distinguishes them from SLOs, which would show a definite ER-TR7+ encapsulation[38].

The role of ATLOs in atherogenesis is still elusive. Nevertheless, atherogenesis-cushioning B1b B cells have been reported as representing the majority of ATLO-derived B cells[39]. This gives rise to the supposition that my identified stage I ATLOs favor the atheroprotective outcome in *Apoe-/- Mif-/-* mice, which gets lost upon aging. As B1 B cells are considered to mediate their atheroprotective functions by producing natural IgM antibodies[26], I determined whether ATLO formation is accompanied by alterations in anti-atherogenic IgM versus pro-atherogenic IgG antibody titers. Both recognize and bind oxidation-specific epitopes (OSEs) like on oxLDL with the difference that anti-oxLDL IgM antibodies block oxLDL internalization by macrophages and foam cell generation, whereas anti-oxLDL IgG antibodies activate macrophages through their Fc receptors and thereby promote lesion formation[27]. Indeed, I measured reduced anti-oxLDL IgM but not anti-oxLDL IgG levels in aged *Apoe-/- Mif-/-* mice, correlating with the lack of the atheroprotective phenotype.

To summarize, the results obtained in this thesis indicate an accelerated generation of adventitial autoimmune B cells upon *Mif*-deficiency, thereby delaying disease progression. The consequent question is whether this effect can be amplified to compensate inflammatory processes during aging.

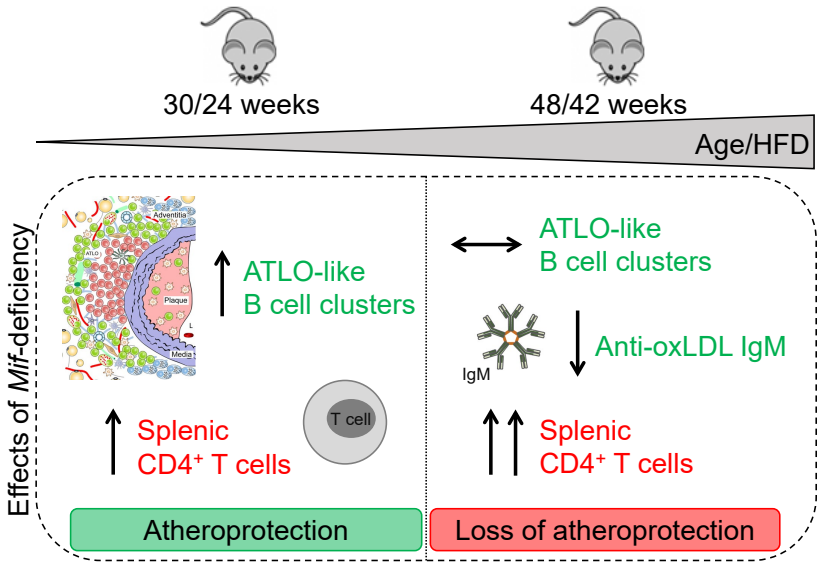


**Figure 21: Schematic overview of MIF- and age-related effects in atherosclerosis.** The atheroprotective phenotype in 30-week-old mice that were set on diet for 24 weeks was accompanied by an accelerated ATLO-like cluster formation and increased CD4+ T cells in the spleen. The loss of atheroprotection in the 48/42-week group was based on rising CD4+ T cells and declining anti-oxLDL IgM antibody levels. Concurrently, ATLO-like cluster build-up was comparable between *Mif*-deficient and *Mif*-proficient mice. Atheroprotective effects are illustrated in green, atheroprogressive effects in red. Figure designed with permission from Yin *et al*., *Front Immunol*, 2016[38].

All considerations are on premise that the data from my mouse models can be translated into humans. Previous studies have unraveled the human CATT repeat polymorphism that effects MIF promoter activity, guiding to a distinction between MIF-low expressers, possessing the CATT5/5 or 5/6 polymorphism, and MIF-high expressers, possessing the CATT6/7 or 7/7 polymorphism[94]. As clinical studies have demonstrated a correlation between MIF expression and carotid artery atherosclerosis[95] as well as complications after cardiac surgery[96], MIF-low expressers might show comparable atheroprotective qualities to the *Mif*-deficient *Apoe-/-* mice in my study. Accordingly, this effect might vanish in advanced age, raising the necessity of effect-prolonging strategies to prevent from severe CVDs. MIF-high expressers seem to be predisposed to early atherosclerosis and therefore require persistent medical check-ups including ultra sound assessment of the carotid arteries and the AA[97,98].

Primary prevention of CVDs focuses on reducing risk factors by lifestyle changes and includes anti-hypertensive, anti-platelet, and lipid-lowering medication[99]. Secondary prevention comprises ß-adrenergic blockers and blood thinners[100,101]. However, great importance should be attached to primary prevention, as advanced atherosclerosis cannot be reversed. Patients taking lipid-lowering medication like statins benefit from

reduced LDL-cholesterol levels and limited oxidation of LDL[102]. Nevertheless, side effects like myopathy or new-onset diabetes mellitus might occur[103].

Considering inflammatory processes, cytokines or chemokines may represent attractive targets for drug development. In fact, the so-called CANTOS trial demonstrated the effectiveness of Canakinumab, an anti-IL-1β antibody, regarding risk reduction of cardiovascular events[104].

As MIF is involved in atherosclerosis, as well as in other inflammatory diseases[64,70,71], metabolic disorders[105,106] and cancer[107,108], MIF-directed approaches, based on antibodies, small molecules, or peptides, have emerged as promising treatment strategies[109-113].

One example would be the monoclonal antibody Imalumab (BAX69) binding to oxidized MIF[114]. A recent phase I study investigated Imalumab in patients with lung, ovarian and colorectal cancer[111]. In addition, the small molecular drug ISO-1 has been demonstrated to bind to the tautomerase region of MIF and to inhibit inflammatory processes in septic mice[112]. However, MIF-targeted interventions might interfere with cardioprotective functions mediated through MIF/CD74[109].

Instead of MIF, MIF receptors can be addressed. For example, CXCR2 and CXCR4 are targeted by small molecules like Reparixin and Plerixafor (AMD3100), respectively[109]. Nevertheless, targeting MIF receptors might limit binding of cognate ligands to their corresponding receptors, such as CXCL8 to CXCR2 and CXCL12 to CXCR4, thereby affecting atheroprotective and homeostatic functions[109].

In contrast, peptides have the potential to selectively target MIF/receptor axes. Recently, a synthetic peptide mimicking the CXCR4 ectodomain (msR4M-L1) was designed to block MIF/CXCR4 interaction without affecting CXCL12/CXCR4 or MIF/D74 signaling. The peptide was able to block arterial leukocyte adhesion *ex vivo*, to reduce atherosclerosis in *Apoe-/-* mice and to bind MIF protein in human carotid endarterectomy lesions[113].

Approaches directed against MIF, MIF receptors, or MIF/receptor axes prove to be promising strategies in atherosclerosis[109,110,113]. However, given the lack of atheroprotection observed in aged global *Apoe-/- Mif-/-* mice, general MIF-blocking mechanisms may be less successful in the elderly as global *Mif* gene deletion or full therapeutic blockade of MIF protein may cause compensatory effects over the course of aging. These could be averted by drug-based blockade of MIF protein for limited times, as opposed to lifelong or genetic. Also, receptor pathway-specific MIF-inhibition might be a viable option. Considering an aging society, age-adjusted strategies are vitally necessary.

In the context of B cells, pro-atherogenic B2 B cells may be considered as therapeutic targets. Accordingly, monoclonal antibodies, aimed at the surface protein CD20, have shown to deplete B2 B cells in atherosclerotic mouse models, thereby reducing plaque development[13,109].

B cell-targeted therapies are well established in various autoimmune diseases including MS, SLE or rheumatoid arthritis[115-117]. Considering the observed changes in plasma anti-oxLDL IgM levels during aging and as a function of MIF, MIF-targeted approaches might provide new opportunities to modulate B cell autoantibody profiles.

# References


1. World Health Organization. Cardiovascular Diseases (CVDs) Fact Sheet. (2021).
2. Weber, C. & Noels, H. Atherosclerosis: current pathogenesis and therapeutic options. *Nat Med* **17**, 1410-1422 (2011).
3. Dahlöf, B. Cardiovascular disease risk factors: epidemiology and risk assessment. *Am J Cardiol* **105**, 3a-9a (2010).
4. Libby, P. Inflammation in atherosclerosis. *Nature* **420**, 868-874 (2002).
5. Hansson, G.K. & Hermansson, A. The immune system in atherosclerosis. *Nat Immunol* **12**, 204-212 (2011).
6. Libby, P., Ridker, P.M. & Hansson, G.K. Progress and challenges in translating the biology of atherosclerosis. *Nature* **473**, 317-325 (2011).
7. Lee, R.T. & Libby, P. The unstable atheroma. *Arterioscler Thromb Vasc Biol* **17**, 1859-1867 (1997).
8. Stöger, J.L.*, et al.* Distribution of macrophage polarization markers in human atherosclerosis. *Atherosclerosis* **225**, 461-468 (2012).
9. Saigusa, R., Winkels, H. & Ley, K. T cell subsets and functions in atherosclerosis. *Nat Rev Cardiol* **17**, 387-401 (2020).
10. Kaartinen, M., Penttilä, A. & Kovanen, P.T. Mast cells in rupture-prone areas of human coronary atheromas produce and store TNF-alpha. *Circulation* **94**, 2787-2792 (1996).
11. Hoffman, W., Lakkis, F.G. & Chalasani, G. B Cells, Antibodies, and More. *Clin J Am Soc Nephrol* **11**, 137-154 (2016).
12. Pieper, K., Grimbacher, B. & Eibel, H. B-cell biology and development. *J Allergy Clin Immunol* **131**, 959-971 (2013).
13. Ait-Oufella, H.*, et al.* B cell depletion reduces the development of atherosclerosis in mice. *J Exp Med* **207**, 1579-1587 (2010).
14. Caligiuri, G., Nicoletti, A., Poirier, B. & Hansson, G.K. Protective immunity against atherosclerosis carried by B cells of hypercholesterolemic mice. *J Clin Invest* **109**, 745-753 (2002).
15. Major, A.S., Fazio, S. & Linton, M.F. B-lymphocyte deficiency increases atherosclerosis in LDL receptor-null mice. *Arterioscler Thromb Vasc Biol* **22**, 1892-1898 (2002).
16. Kyaw, T.*, et al.* Conventional B2 B cell depletion ameliorates whereas its adoptive transfer aggravates atherosclerosis. *J Immunol* **185**, 4410-4419 (2010).
17. Srikakulapu, P. & McNamara, C.A. B cells and atherosclerosis. *Am J Physiol Heart Circ Physiol* **312**, H1060-h1067 (2017).
18. LeBien, T.W. & Tedder, T.F. B lymphocytes: how they develop and function. *Blood* **112**, 1570-1580 (2008).
19. Weller, S.*, et al.* Human blood IgM "memory" B cells are circulating splenic marginal zone B cells harboring a prediversified immunoglobulin repertoire. *Blood* **104**, 3647-3654 (2004).
20. Hayakawa, K., Hardy, R.R., Herzenberg, L.A. & Herzenberg, L.A. Progenitors for Ly-1 B cells are distinct from progenitors for other B cells. *J Exp Med* **161**, 1554-1568 (1985).
21. Mandel, E.M. & Grosschedl, R. Transcription control of early B cell differentiation. *Curr Opin Immunol* **22**, 161-167 (2010).
22. Cambier, J.C., Gauld, S.B., Merrell, K.T. & Vilen, B.J. B-cell anergy: from transgenic models to naturally occurring anergic B cells? *Nat Rev Immunol* **7**, 633-643 (2007).
23. Melchers, F. Checkpoints that control B cell development. *J Clin Invest* **125**, 2203-2210 (2015).

24. Batten, M.*, et al.* BAFF mediates survival of peripheral immature B lymphocytes. *J Exp Med* **192**, 1453-1466 (2000).

25. Pillai, S. & Cariappa, A. The follicular versus marginal zone B lymphocyte cell fate decision. *Nat Rev Immunol* **9**, 767-777 (2009).

26. Kyaw, T.*, et al.* B1a B lymphocytes are atheroprotective by secreting natural IgM that increases IgM deposits and reduces necrotic cores in atherosclerotic lesions. *Circ Res* **109**, 830-840 (2011).

27. Tsiantoulas, D., Diehl, C.J., Witztum, J.L. & Binder, C.J. B cells and humoral immunity in atherosclerosis. *Circ Res* **114**, 1743-1756 (2014).

28. Rosenfeld, S.M.*, et al.* B-1b Cells Secrete Atheroprotective IgM and Attenuate Atherosclerosis. *Circ Res* **117**, e28-39 (2015).

29. Oliver, A.M., Martin, F., Gartland, G.L., Carter, R.H. & Kearney, J.F. Marginal zone B cells exhibit unique activation, proliferative and immunoglobulin secretory responses. *Eur J Immunol* **27**, 2366-2374 (1997).

30. Nus, M.*, et al.* Marginal zone B cells control the response of follicular helper T cells to a high-cholesterol diet. *Nat Med* **23**, 601-610 (2017).

31. Strom, A.C.*, et al.* B regulatory cells are increased in hypercholesterolaemic mice and protect from lesion development via IL-10. *Thromb Haemost* **114**, 835-847 (2015).

32. Centa, M.*, et al.* Germinal Center-Derived Antibodies Promote Atherosclerosis Plaque Size and Stability. *Circulation* **139**, 2466-2482 (2019).

33. Hilgendorf, I.*, et al.* Innate response activator B cells aggravate atherosclerosis by stimulating T helper-1 adaptive immunity. *Circulation* **129**, 1677-1687 (2014).

34. Zhou, X. & Hansson, G.K. Detection of B cells and proinflammatory cytokines in atherosclerotic plaques of hypercholesterolaemic apolipoprotein E knockout mice. *Scand J Immunol* **50**, 25-30 (1999).

35. Moos, M.P.*, et al.* The lamina adventitia is the major site of immune cell accumulation in standard chow-fed apolipoprotein E-deficient mice. *Arterioscler Thromb Vasc Biol* **25**, 2386-2391 (2005).

36. Weih, F., Gräbner, R., Hu, D., Beer, M. & Habenicht, A.J. Control of dichotomic innate and adaptive immune responses by artery tertiary lymphoid organs in atherosclerosis. *Front Physiol* **3**, 226 (2012).

37. Mohanta, S.K.*, et al.* Artery tertiary lymphoid organs contribute to innate and adaptive immune responses in advanced mouse atherosclerosis. *Circ Res* **114**, 1772-1787 (2014).

38. Yin, C., Mohanta, S.K., Srikakulapu, P., Weber, C. & Habenicht, A.J. Artery Tertiary Lymphoid Organs: Powerhouses of Atherosclerosis Immunity. *Front Immunol* **7**, 387 (2016).

39. Srikakulapu, P.*, et al.* Artery Tertiary Lymphoid Organs Control Multilayered Territorialized Atherosclerosis B-Cell Responses in Aged ApoE-/- Mice. *Arterioscler Thromb Vasc Biol* **36**, 1174-1185 (2016).

40. Murphy, P.M.*, et al.* International union of pharmacology. XXII. Nomenclature for chemokine receptors. *Pharmacol Rev* **52**, 145-176 (2000).

41. Fernandez, E.J. & Lolis, E. Structure, function, and inhibition of chemokines. *Annu Rev Pharmacol Toxicol* **42**, 469-499 (2002).

42. Rajagopalan, L. & Rajarathnam, K. Structural basis of chemokine receptor function--a model for binding affinity and ligand selectivity. *Biosci Rep* **26**, 325-339 (2006).

43. Thelen, M. Dancing to the tune of chemokines. *Nat Immunol* **2**, 129-134 (2001).

44. Zernecke, A. & Weber, C. Chemokines in atherosclerosis: proceedings resumed. *Arterioscler Thromb Vasc Biol* **34**, 742-750 (2014).

45. Tacke, F.*, et al.* Monocyte subsets differentially employ CCR2, CCR5, and CX3CR1 to accumulate within atherosclerotic plaques. *J Clin Invest* **117**, 185-194 (2007).

46. Soehnlein, O.*, et al.* Distinct functions of chemokine receptor axes in the atherogenic mobilization and recruitment of classical monocytes. *EMBO Mol Med* **5**, 471-481 (2013).

47. Drechsler, M., Megens, R.T., van Zandvoort, M., Weber, C. & Soehnlein, O. Hyperlipidemia-triggered neutrophilia promotes early atherosclerosis. *Circulation* **122**, 1837-1845 (2010).

48. Zernecke, A.*, et al.* Protective role of CXC receptor 4/CXC ligand 12 unveils the importance of neutrophils in atherosclerosis. *Circ Res* **102**, 209-217 (2008).

49. Kapurniotu, A., Gokce, O. & Bernhagen, J. The Multitasking Potential of Alarmins and Atypical Chemokines. *Front Med (Lausanne)* **6**, 3 (2019).

50. Bernhagen, J.*, et al.* Purification, bioactivity, and secondary structure analysis of mouse and human macrophage migration inhibitory factor (MIF). *Biochemistry* **33**, 14144-14155 (1994).

51. David, J.R. Delayed hypersensitivity in vitro: its mediation by cell-free substances formed by lymphoid cell-antigen interaction. *Proc Natl Acad Sci U S A* **56**, 72-77 (1966).

52. Mischke, R., Kleemann, R., Brunner, H. & Bernhagen, J. Cross-linking and mutational analysis of the oligomerization state of the cytokine macrophage migration inhibitory factor (MIF). *FEBS Lett* **427**, 85-90 (1998).

53. Sun, H.W., Bernhagen, J., Bucala, R. & Lolis, E. Crystal structure at 2.6-A resolution of human macrophage migration inhibitory factor. *Proc Natl Acad Sci U S A* **93**, 5191-5196 (1996).

54. Pawig, L., Klasen, C., Weber, C., Bernhagen, J. & Noels, H. Diversity and Inter-Connections in the CXCR4 Chemokine Receptor/Ligand Family: Molecular Perspectives. *Front Immunol* **6**, 429 (2015).

55. Tillmann, S., Bernhagen, J. & Noels, H. Arrest Functions of the MIF Ligand/Receptor Axes in Atherogenesis. *Front Immunol* **4**, 115 (2013).

56. Merk, M., Mitchell, R.A., Endres, S. & Bucala, R. D-dopachrome tautomerase (D-DT or MIF-2): doubling the MIF cytokine family. *Cytokine* **59**, 10-17 (2012).

57. Baugh, J.A. & Bucala, R. Macrophage migration inhibitory factor. *Crit Care Med* **30**, S27-35 (2002).

58. Chen, L.*, et al.* Induction of MIF expression by oxidized LDL via activation of NF-kappaB in vascular smooth muscle cells. *Atherosclerosis* **207**, 428-433 (2009).

59. Nishihira, J., Koyama, Y. & Mizue, Y. Identification of macrophage migration inhibitory factor (MIF) in human vascular endothelial cells and its induction by lipopolysaccharide. *Cytokine* **10**, 199-205 (1998).

60. Flieger, O.*, et al.* Regulated secretion of macrophage migration inhibitory factor is mediated by a non-classical pathway involving an ABC transporter. *FEBS Lett* **551**, 78-86 (2003).

61. Lue, H., Kleemann, R., Calandra, T., Roger, T. & Bernhagen, J. Macrophage migration inhibitory factor (MIF): mechanisms of action and role in disease. *Microbes Infect* **4**, 449-460 (2002).

62. Jankauskas, S.S., Wong, D.W.L., Bucala, R., Djudjaj, S. & Boor, P. Evolving complexity of MIF signaling. *Cell Signal* **57**, 76-88 (2019).

63. Leng, L.*, et al.* MIF signal transduction initiated by binding to CD74. *J Exp Med* **197**, 1467-1476 (2003).

64. Bernhagen, J.*, et al.* MIF is a noncognate ligand of CXC chemokine receptors in inflammatory and atherogenic cell recruitment. *Nat Med* **13**, 587-596 (2007).

65. Lue, H., Dewor, M., Leng, L., Bucala, R. & Bernhagen, J. Activation of the JNK signalling pathway by macrophage migration inhibitory factor (MIF) and dependence on CXCR4 and CD74. *Cell Signal* **23**, 135-144 (2011).

66. Li, A., Dubey, S., Varney, M.L., Dave, B.J. & Singh, R.K. IL-8 directly enhanced endothelial cell survival, proliferation, and matrix metalloproteinases production and regulated angiogenesis. *J Immunol* **170**, 3369-3376 (2003).

67. Mitchell, R.A., Metz, C.N., Peng, T. & Bucala, R. Sustained mitogen-activated protein kinase (MAPK) and cytoplasmic phospholipase A2 activation by macrophage migration inhibitory factor (MIF). Regulatory role in cell proliferation and glucocorticoid action. *J Biol Chem* **274**, 18100-18106 (1999).

68. Gore, Y.*, et al.* Macrophage migration inhibitory factor induces B cell survival by activation of a CD74-CD44 receptor complex. *J Biol Chem* **283**, 2784-2792 (2008).

69. Merk, M.*, et al.* The D-dopachrome tautomerase (DDT) gene product is a cytokine and functional homolog of macrophage migration inhibitory factor (MIF). *Proc Natl Acad Sci U S A* **108**, E577-585 (2011).

70. Calandra, T. & Roger, T. Macrophage migration inhibitory factor: a regulator of innate immunity. *Nat Rev Immunol* **3**, 791-800 (2003).

71. Leech, M.*, et al.* Macrophage migration inhibitory factor in rheumatoid arthritis: evidence of proinflammatory function and regulation by glucocorticoids. *Arthritis Rheum* **42**, 1601-1608 (1999).

72. Burger-Kentischer, A.*, et al.* Expression of macrophage migration inhibitory factor in different stages of human atherosclerosis. *Circulation* **105**, 1561-1566 (2002).

73. Müller, II*, et al.* Macrophage migration inhibitory factor is enhanced in acute coronary syndromes and is associated with the inflammatory response. *PLoS One* **7**, e38376 (2012).

74. Pan, J.H.*, et al.* Macrophage migration inhibitory factor deficiency impairs atherosclerosis in low-density lipoprotein receptor-deficient mice. *Circulation* **109**, 3149-3153 (2004).

75. Schober, A.*, et al.* Stabilization of atherosclerotic plaques by blockade of macrophage migration inhibitory factor after vascular injury in apolipoprotein E-deficient mice. *Circulation* **109**, 380-385 (2004).

76. Atsumi, T., Nishihira, J., Makita, Z. & Koike, T. Enhancement of oxidised low-density lipoprotein uptake by macrophages in response to macrophage migration inhibitory factor. *Cytokine* **12**, 1553-1556 (2000).

77. Kong, Y.Z.*, et al.* Macrophage migration inhibitory factor induces MMP-9 expression: implications for destabilization of human atherosclerotic plaques. *Atherosclerosis* **178**, 207-215 (2005).

78. Miller, E.J.*, et al.* Macrophage migration inhibitory factor stimulates AMP-activated protein kinase in the ischaemic heart. *Nature* **451**, 578-582 (2008).

79. Klasen, C.*, et al.* MIF promotes B cell chemotaxis through the receptors CXCR4 and CD74 and ZAP-70 signaling. *J Immunol* **192**, 5273-5284 (2014).

80. Matza, D., Wolstein, O., Dikstein, R. & Shachar, I. Invariant chain induces B cell maturation by activating a TAF(II)105-NF-kappaB-dependent transcription program. *J Biol Chem* **276**, 27203-27206 (2001).

81. Klasen, C.*, et al.* LPS-mediated cell surface expression of CD74 promotes the proliferation of B cells in response to MIF. *Cell Signal* **46**, 32-42 (2018).

82. Lapter, S.*, et al.* A role for the B-cell CD74/macrophage migration inhibitory factor pathway in the immunomodulation of systemic lupus erythematosus by a therapeutic tolerogenic peptide. *Immunology* **132**, 87-95 (2011).

83. Alampour-Rajabi, S.*, et al.* MIF interacts with CXCR7 to promote receptor internalization, ERK1/2 and ZAP-70 signaling, and lymphocyte chemotaxis. *Faseb j* **29**, 4497-4511 (2015).

84. Rijvers, L.*, et al.* The macrophage migration inhibitory factor pathway in human B cells is tightly controlled and dysregulated in multiple sclerosis. *Eur J Immunol* **48**, 1861-1871 (2018).

85. Schmitz, C.*, et al.* Mif-deficiency favors an atheroprotective autoantibody phenotype in atherosclerosis. *Faseb j* **32**, 4428-4443 (2018).

86. Fingerle-Rowson, G.*, et al.* The p53-dependent effects of macrophage migration inhibitory factor revealed by gene targeting. *Proc Natl Acad Sci U S A* **100**, 9354-9359 (2003).

87. Chen, Z.*, et al.* Evidence for a role of macrophage migration inhibitory factor in vascular disease. *Arterioscler Thromb Vasc Biol* **24**, 709-714 (2004).

88. Burger-Kentischer, A.*, et al.* Reduction of the aortic inflammatory response in spontaneous atherosclerosis by blockade of macrophage migration inhibitory factor (MIF). *Atherosclerosis* **184**, 28-38 (2006).

89. Krammer, C.*, et al.* Pathways linking aging and atheroprotection in Mif-deficient atherosclerotic mice. *Faseb j* **37**, e22752 (2023).

90. Smykiewicz, P., Segiet, A., Keag, M. & Żera, T. Proinflammatory cytokines and ageing of the cardiovascular-renal system. *Mech Ageing Dev* **175**, 35-45 (2018).

91. Tyrrell, D.J. & Goldstein, D.R. Ageing and atherosclerosis: vascular intrinsic and extrinsic factors and potential role of IL-6. *Nat Rev Cardiol* **18**, 58-68 (2021).

92. Lefebvre, J.S.*, et al.* The aged microenvironment contributes to the age-related functional defects of CD4 T cells in mice. *Aging Cell* **11**, 732-740 (2012).

93. Masters, A.R., Jellison, E.R., Puddington, L., Khanna, K.M. & Haynes, L. Attrition of T Cell Zone Fibroblastic Reticular Cell Number and Function in Aged Spleens. *Immunohorizons* **2**, 155-163 (2018).

94. Baugh, J.A.*, et al.* A functional promoter polymorphism in the macrophage migration inhibitory factor (MIF) gene associated with disease severity in rheumatoid arthritis. *Genes Immun* **3**, 170-176 (2002).

95. Lan, M.Y.*, et al.* Association between MIF gene polymorphisms and carotid artery atherosclerosis. *Biochem Biophys Res Commun* **435**, 319-322 (2013).

96. Averdunk, L.*, et al.* The Macrophage Migration Inhibitory Factor (MIF) Promoter Polymorphisms (rs3063368, rs755622) Predict Acute Kidney Injury and Death after Cardiac Surgery. *J Clin Med* **9**(2020).

97. Spanos, K.*, et al.* Carotid Bifurcation Geometry as Assessed by Ultrasound is Associated with Early Carotid Atherosclerosis. *Ann Vasc Surg* **51**, 207-216 (2018).

98. Parkkila, K.*, et al.* Abdominal aorta plaques are better in predicting future cardiovascular events compared to carotid intima-media thickness: A 20-year prospective study. *Atherosclerosis* **330**, 36-42 (2021).

99. Stewart, J., Addy, K., Campbell, S. & Wilkinson, P. Primary prevention of cardiovascular disease: Updated review of contemporary guidance and literature. *JRSM Cardiovasc Dis* **9**, 2048004020949326 (2020).

100. Sipahi, I.*, et al.* Beta-blockers and progression of coronary atherosclerosis: pooled analysis of 4 intravascular ultrasonography trials. *Ann Intern Med* **147**, 10-18 (2007).

101. Ittaman, S.V., VanWormer, J.J. & Rezkalla, S.H. The role of aspirin in the prevention of cardiovascular disease. *Clin Med Res* **12**, 147-154 (2014).

102. Rosenson, R.S. Statins in atherosclerosis: lipid-lowering agents with antioxidant capabilities. *Atherosclerosis* **173**, 1-12 (2004).

103. Collins, R.*, et al.* Interpretation of the evidence for the efficacy and safety of statin therapy. *Lancet* **388**, 2532-2561 (2016).

104. Ridker, P.M.*, et al.* Antiinflammatory Therapy with Canakinumab for Atherosclerotic Disease. *N Engl J Med* **377**, 1119-1131 (2017).

105. Yabunaka, N.*, et al.* Elevated serum content of macrophage migration inhibitory factor in patients with type 2 diabetes. *Diabetes Care* **23**, 256-258 (2000).

106. Church, T.S.*, et al.* Obesity, macrophage migration inhibitory factor, and weight loss. *Int J Obes (Lond)* **29**, 675-681 (2005).

107. Meyer-Siegler, K. & Hudson, P.B. Enhanced expression of macrophage migration inhibitory factor in prostatic adenocarcinoma metastases. *Urology* **48**, 448-452 (1996).

108. Agarwal, R.*, et al.* Macrophage migration inhibitory factor expression in ovarian cancer. *Am J Obstet Gynecol* **196**, 348.e341-345 (2007).

109. Sinitski, D.*, et al.* Macrophage Migration Inhibitory Factor (MIF)-Based Therapeutic Concepts in Atherosclerosis and Inflammation. *Thromb Haemost* **119**, 553-566 (2019).

110. Krammer, C.*, et al.* A MIF-Derived Cyclopeptide that Inhibits MIF Binding and Atherogenic Signaling via the Chemokine Receptor CXCR2. *Chembiochem* **22**, 1012-1019 (2021).

111. Mahalingam, D.*, et al.* Phase I study of imalumab (BAX69), a fully human recombinant antioxidized macrophage migration inhibitory factor antibody in advanced solid tumours. *Br J Clin Pharmacol* **86**, 1836-1848 (2020).

112. Al-Abed, Y.*, et al.* ISO-1 binding to the tautomerase active site of MIF inhibits its pro-inflammatory activity and increases survival in severe sepsis. *J Biol Chem* **280**, 36541-36544 (2005).

113. Kontos, C.*, et al.* Designed CXCR4 mimic acts as a soluble chemokine receptor that blocks atherogenic inflammation by agonist-specific targeting. *Nat Commun* **11**, 5981 (2020).

114. Schinagl, A.*, et al.* Role of the Cysteine 81 Residue of Macrophage Migration Inhibitory Factor as a Molecular Redox Switch. *Biochemistry* **57**, 1523-1532 (2018).

115. Nguyen, A.L., Gresle, M., Marshall, T., Butzkueven, H. & Field, J. Monoclonal antibodies in the treatment of multiple sclerosis: emergence of B-cell-targeted therapies. *Br J Pharmacol* **174**, 1895-1907 (2017).

116. Bag-Ozbek, A. & Hui-Yuen, J.S. Emerging B-Cell Therapies in Systemic Lupus Erythematosus. *Ther Clin Risk Manag* **17**, 39-54 (2021).

117. Wu, F.*, et al.* B Cells in Rheumatoid Arthritis : Pathogenic Mechanisms and Treatment Prospects. *Front Immunol* **12**, 750753 (2021).

# List of Publications

Krammer C, Yang B, **Reichl S**, Besson-Girard S, Ji H, Bolini V, Schulte C, Noels H, Schlepckow K, Jocher G, Werner G, Willem M, El Bounkari O, Kapurniotu A, Gokce O, Weber C, Mohanta S, Bernhagen J. Pathways linking aging and atheroprotection in *Mif*-deficient atherosclerotic mice. ***FASEB J.*** 2023 Mar;37(3):e22752.

# Danksagung

Die vorliegende Doktorarbeit wurde am Lehrstuhl für Vaskuläre Biologie des Instituts für Schlaganfall- und Demenzforschung (ISD) angefertigt und durch das Förderprogramm für Forschung und Lehre (FöFoLe) der Ludwig-Maximilians-Universität (LMU) München unterstützt. An dieser Stelle möchte ich mich bei allen Personen bedanken, die zum Erfolg dieser Arbeit beigetragen haben.

Besonderer Dank gilt Herrn Univ.-Prof. Dr. rer. nat. Jürgen Bernhagen, der es mir ermöglichte, meine Arbeit unter seiner Supervision anzufertigen und Teil eines engagierten internationalen Teams zu sein. Ich schätze seine kontinuierliche Unterstützung, seinen wissenschaftlichen Input sowie die anregenden Gespräche, die wir in den vergangenen Jahren geführt haben. Ohne ihn wäre der Erfolg meiner Untersuchungen, die neue Erkenntnisse über MIF im Kontext der B-Zell-Rekrutierung bei der Atherogenese darlegen, nicht denkbar gewesen.

Ich möchte meinen größten Respekt an Frau Dr. rer. nat. Christine Krammer aussprechen, die neben ihrem eigenen Promotionsstudium, eine exzellente Betreuung gewährleistet hat. Ich bedanke mich für die enorme Hilfe bei der Planung und Durchführung von Versuchen und bei der Lösung von Problemen. Die Etablierung sämtlicher in dieser Arbeit angewandten Methoden wäre mir ohne sie kaum möglich gewesen.

Außerdem danke ich Herrn Dr. rer. nat. Omar El Bounkari für die stetige Unterstützung und die zahlreichen Ratschläge, die erheblich zum Gelingen meiner Experimente beigetragen haben.

Ich möchte mich auch bei Frau Bishan Yang und Frau Verena Bolini bedanken, die an der Quantifizierung atherosklerotischer Plaques in *Mif*-defizienten versus *Mif*-exprimierenden *Apoe-/-* Mäusen beteiligt waren, sowie bei Frau Priscila Bourilhón und Frau Simona Gerra für ihre Assistenz im Laboralltag.

Darüber hinaus bedanke mich bei allen anderen Mitgliedern der AG Bernhagen und AG Gökçe für zahlreiche konstruktive Diskussionen, die Hilfsbereitschaft und die angenehme Arbeitsatmosphäre. Ich hatte eine sehr schöne Zeit, an die ich mich gerne zurückerinnere.

Ich bedanke mich beim gesamten Team der ISD Animal Facility für die gewissenhafte Pflege unserer Mäuse und den Support bei allen Fragen bezüglich der tierexperimentellen Arbeit.

Des Weiteren möchte ich Herrn Univ.-Prof. Dr. med. Thomas Gudermann, Vorstand des Förderprogramms für Forschung und Lehre (FöFoLe), und der medizinischen Fakultät der LMU für die wissenschaftliche Ausbildung und die Finanzierung des Projekts danken.

Zu guter Letzt geht ein großes Dankeschön an meine Eltern und meine beiden Schwestern, die mir den nötigen Rückhalt gaben und mich immer ermutigten, wenn es Schwierigkeiten gab.

# Affidavit


**Eidesstattliche Versicherung**

Reichl, Sabrina

Name, Vorname

Ich erkläre hiermit an Eides statt, dass ich die vorliegende Dissertation mit dem Titel:

**The atypical chemokine MIF and B lymphocytes in atherosclerosis: emerging molecular and cellular links**

selbständig verfasst, mich außer der angegebenen keiner weiteren Hilfsmittel bedient und alle Erkenntnisse, die aus dem Schrifttum ganz oder annähernd übernommen sind, als solche kenntlich gemacht und nach ihrer Herkunft unter Bezeichnung der Fundstelle einzeln nachgewiesen habe.

Ich erkläre des Weiteren, dass die hier vorgelegte Dissertation nicht in gleicher oder in ähnlicher Form bei einer anderen Stelle zur Erlangung eines akademischen Grades eingereicht wurde.

Zürich, 11.12.2023

Ort, Datum

Sabrina Reichl

Unterschrift Doktorandin